A Thesis

entitled

Formulating an Essential Oil Extracted from Monodora myristica into a Tablet That Forms In-situ Nanostructured Dispersions.

by

Elizabeth Oladoyin Agboluaje

Submitted to the Graduate Faculty as partial fulfillment of the requirements for the Master of Science Degree in Pharmaceutical Sciences:

Industrial Pharmacy

_____

Jerry Nesamony, PHD., Committee Chair

_____

Gabriella Baki, PHD., Committee Member

_____

Tillekeratne, Liyanaaratchige, PHD., Committee Member

_____

Barry Scheuermann, Ph.D., Interim Dean
College of Graduate Studies

The University of Toledo

May 2021

An Abstract of

Formulating an Essential Oil Extracted from Monodora myristica into a Tablet That Forms In-situ Nanostructured Dispersions.

by

Elizabeth Oladoyin Agboluaje

Submitted to the Graduate Faculty as partial fulfillment of the requirements for the Master of Science Degree in
Pharmaceutical Science, Industrial Pharmacy

The University of Toledo
May 2021

Self-micro-emulsifying drug delivery systems (SMEDDS) have been proven to have improved drug stability, lower toxicity, and increase bioavailability of insoluble drugs. It is a drug delivery design that can prevent physical and chemical drug degradation. The goal of this study was to develop a solid formulation incorporating a self-micro-emulsifying drug delivery system (SMEDDS) for the oral delivery of *Monodora myristica* essential oil (MMEO). MMEO was extracted from the blended seeds of *Monodora myristica* using the hydro-distillation method. MMEO was characterized by evaluating the physicochemical properties to ascertain the quality and purity of the essential oil by comparing with MMEO data in the literature. The design of the experiment was done by using Fusion Pro by S-Matrix (Fusion Pro Software Version 9.9.0 Build690, S-Matrix Corporation (www.smatrix.com)) to compare a combination of MMEO/Tween 80/Transcutol HP and MMEO/ Kolliphor/ Labrasol 12 formulations. MMEO (10.92%) / Tween 80 (48%) /Transcutol HP (41.8%) was predicted to be the best formulation with desirable characteristics such as a mean particle size of 112.7 nm, the zeta potential of +5.10 mv, and a transparent emulsion. The emulsion formed was stable over 90 days without any

form of emulsion instability or oil precipitation. The liquid-SMEDDS was adsorbed unto Neusilin US2 to form solid-SMEDDS. The solid-SMEDDS was added to cellulose, lactose, starch, talc, magnesium stearate to directly compress type 1 and type 2 tablets while the solid-SMEDDS was directly compressed to formulate type 3 tablets. Type 3 tablets had the highest drug loading capacity unlike type 1 and type 2 tablets. Also, type 3 had the highest breaking force and longest disintegration time. Using one-way ANOVA, the P-value obtained was below 0.05 for tablet thickness, tablet breaking force, and disintegration tests. Therefore, there was a statistically significant difference between type 1, type 2, and type 3 tablets properties such as tablet thickness (<0.001), tablet breaking force (<0.001), and disintegration time (<0.001). The p-value for the % friability (0.081) was above 0.05. Thus, there is no significant difference in the % weight loss for type 1, type 2, and type 3 tablets. A tablet-loaded SMEDDS formulation is a promising approach to deliver essential oils (water poorly soluble drugs). Excipients such as cellulose, starch, lactose, talc, magnesium stearate did not improve the physicochemical properties of type 1 and type 2 tablets. Based on data obtained from this study, it may be concluded that type 3 tablet design should be adopted for further studies. Solid-SMEDDS may also be filled into capsule shells and comparative studies can be done with type 3 tablets. In-vivo bioavailability studies can also be done to better evaluate the type-3 tablets. Animal studies to test for the pharmacology properties like; Alzheimer, anticancer, antioxidant, and antimicrobial properties of the formulation will provide information about the utility of MMEO as a therapeutic agent.

Acknowledgment

Truly, every great journey starts with the first step. I would love to deeply appreciate God who has been intentional with my life and He strategically placed people in the path of my destiny. Having Dr. Jerry Nesamony as my research advisor has been greatly instrumental to my academic growth at the University of Toledo. He has taught me to how to be an independent scientist, critically have thought-provoking scientific discussions, and be a self-motivated student. His impact on my life would always be treasured.

I would like to appreciate Dr.Liyanaaratchige Tillekeratne ; my thesis committee member who at the beginning of this research provided all the oil extraction instruments for me and trained me on how to properly perform oil extraction. I am sincerely thankful to Dr. Gabriella Baki, my thesis committee member also for her constant words of encouragement and support over the past two years. I thank Fuji Chemical Industries for providing samples of neusilin US2. I would also like to thank Gatteffose corporation for providing me with Transcutol HP and Labrasol. To my colleagues, Subah Farah and Briana Maktabi, this journey was more awesome working with you in the laboratory. Home will always be where the heart is. I would never forget the great impacts of my parents, HRH Cornelius Agboluaje and HRM Roseline Agboluaje on my life. A shoutout to my sisters for their continued support. I hope I always make you proud. To my best friend, Jim Omodolapo thanks for doing life with me.

Table of Contents

List of Tables

List of Figures

List of Abbreviations

DOE…….Design of Experiment

DNA.....……..Deoxyribonucleic Acid

HLB……..Hydrophilic-lipophilic Balance

HCL…….Hydrochloric Acid

(KOH)……Potassium Hydroxide

M.myristica……..*Monodora Myristica*

MMEO …….. *Monodora Myristica* Essential Oil

NAOH……Sodium Hydroxide

SEDDS…….Self-emulsifying Drug Delivery System

SMEDDS……Self-micro-emulsifying Drug Delivery System

SNEDDS……...Self-nano-emulsifying Drug Delivery System

UV-VIS Spectrophotometer …….Ultraviolet-Visible Spectrophotometer

List of Symbols

α……...Angle of incidence
β .....Angle of distortion

° .....Degrees
°C .....Degree Celcius

Chapter 1

Introduction

1.1. *Monodora myristica*

Before the advances in technology and industrial promotion, mankind had been solely dependent on plants for the treatment of ailments and diseases all over the world (2). Over the past few years, there has been a recent refocus on plants for medicinal purposes to maximize the numerous pharmacology effects they possess. One of such plants that has great medicinal potentials but has not been intensively studied is called *Monodora myristica*; a tropical plant from the Annonaceae family. The English names for this plant also include African, Jamaica, and calabash nutmeg(3). This plant is widely populated in Sub-Saharan Africa and can also be found in Australia, Asia, Central and South America (4). The seed of *Monodora myristica* is commonly used as a food spice and condiment in Africa. There has been a lot of ethnomedicinal uses of various parts of this plant over centuries. The bark has been used to treat piles, eye problems, fevers, and stomachaches (5) (Erukainure, 2018 #27). The seeds have been used as a stimulant in snuffs in West Africa, management of hypertension, headaches, constipation, and uterine hemorrhage after childbirth in women, etc.(5),(6). The pomade form of the plant can be used for lice and fleas' treatments and sores in general as reported in Gabon. The seeds have also been reported to be effective as an emetic agent (7). The constituents of the seeds include;

flavonoids, terpenes, tannins, saponins, anthraquinones, resins, alkaloids, arocine, sterols, and cyanogenic glycosides (4). Some of the specific compounds that have been identified by gas chromatography-mass spectrophotometry include; α-limonene (beneficial for cancer prevention and treatment, weight loss and bronchitis treatment), germacrenes (acts as antimicrobial and anti-insecticidal), cis oleic acid, and oleic acid (excellent emollient properties), myrcene, caryophyllene, α-phellandrene, α-pinene, α- humulene, eugenol, elemicin, and α-pinene(4).

The scientifically proven pharmacological use of the seeds include the following:

1. Antioxidant properties: Free radicals sometimes exist in the body which can be injurious to cells. The formation of reactive oxygen species can be caused by air pollutants, exposure to X-rays, and hazardous chemicals. Free radicals are involved in the development of cancer, Alzheimer‘s diseases, hypertension, diabetes mellites, DNA damage, and liver damage. The flavonoid and phenolic content of *M. myristica* seed have been proven to have significant antioxidant effects (8).
2. Antidepressant properties: A recent study showed that the essential oil of *M. myristica* seed can be used both in the management and treatment of depression. A chronic unpredictable mild stress was induced in rats and the behavioral pattern was studied after the administration of M.myristica essential oil. Biochemical parameters were also studied, and it was reported that significant amelioration of the depression was observed with MMEO (150 and 300 mg/kg body weight). The antidepressant effect was said to be comparable with fluoxetine (Prozac ™). The mechanism of action was reported to be through the pathway of serum

Corticosterone (CORT) and brain Monoamine Oxidase-A (MAO-A) levels reduction (9).

3. Alzheimer's Treatment: MMEO is effective against the management and treatment of Alzheimer's diseases. The mechanism of action is by MMEO acting as acetylcholinesterase inhibitor thereby increasing the amount of acetylcholine present. This was done using Ellman's colorimetric method and the inhibitory activity was compared to galantamine's acetylcholine inhibitory activity (10).
4. Anti-sickling properties: Sickled erythrocytes were treated with acetone extract of *M.myristica* at 37°C for 6, 12, and 24 hours. Antioxidative analysis was then done by checking for reduced glutathione (GSH), catalase, and lipid peroxidation. The mechanism of action involves the molecular interaction of acetone extract of *M.myristica* with α-dimer of Hemoglobin. 17-octadecenoic acid and oleic acid were the major compounds responsible for the anti-sickling effect(6).
5. Anti-inflammatory properties: *M. myristica* seed extract has also been proven to be effective against inflammation in the body. Inflammation is a natural biological response to unwanted stimuli. Inflammation causes swelling and pain. The anti-inflammatory property of MMEO has been attributed to its high flavonoid component. The mechanism of action has been proposed to be modulation of enzymes like cyclooxygenase, phospholipase A2, lipoxygenase which then ultimately reduces the production of inflammatory mediators (prostaglandins, and leukotrienes,)(11).

Other scientifically proven pharmacology effects of *M myristica* include prevention and management of cancer, anti-emetic, cardioprotective, and management of diabetes

mellitus. The numerous benefits of this seed have made it an interesting plant for mankind. It has been reported in nature that some medicinal plants constituent shows the synergistic medicinal effect and the effects tend to wane down when separated. A group recently isolated a novel cyclopropane fatty acid compound called 13-(2-butylcyclopropyl)-6,9-dodecanoic acid by liquid chromatography-mass spectrophotometry analysis and nuclear magnetic resonance analysis(12).

Figure 1-1. *Monodora myristica* Unpeeled Seed Picture (13)

Figure 1-2. *Monodora myristica* peeled Seed Picture(13)

1.2. Self-Micro Emulsifying Drug Delivery Systems (SMEDSS)

The majority of essential oils have been classified to be insoluble in water and this impedes the formulation designs. Some of the methods that can be used to deliver water-insoluble drugs include lipid-based formulations, crystalline solids micronization, and amorphous formulations. The lipid-based formulation has gained huge popularity for essential oils. (14). It has been proven that lipid-based formulations possess higher bioavailability due to their ability to bypass passage into the hepatic portal vein and evade hepatic degradation. Evasion is said to occur through the Peyer's patch (15). Various classes of lipid-based formulations consist of macroemulsion, microemulsion, self-emulsifying drug delivery system (SEDDS), liposomes, lipoplexes, and solid-lipid nanoparticles. Emulsions can be described as a combination of two mixtures; with a dispersed phase and a continuous phase with a third liquid to act as an emulsifier. Sometimes, other ingredients such as a co-solvent or a preservative due to the water content can be included. Emulsions can be oil in water or water in oil emulsion or multiple emulsion (W/O/W or O/W/O) (14) (16). Self-emulsifying drug delivery systems (SEDDS) can be self-micro emulsifying drug delivery systems (SMEDDS) or self-nano emulsifying drug delivery systems (SNEDDS). SEDDS are isotropic mixtures of oil, surfactants, and sometimes co-surfactant (17). SEDDS transform into emulsion in the gastrointestinal tract under gentle agitation produced by peristalsis. Self-emulsification is better achieved when there is ultra-low-water interfacial tension and disruption (18). With SEDDS, dilution can lead to nano-microemulsion with an expected mean particle size of 20 and 200nm. The word nano-emulsions and microemulsions have been used interchangeably by a lot of scientists but they are differentiated by the method of preparation (19). SMEDDS has the added advantage of

offering large interfacial surface areas thereby which increases drug partitioning. The major difference between SEDDS, SMEDDS, and SNEDDS can be seen in table 1.1(20).

Table 1. 1. Distinct Characteristics between SEDDS, SMEDDS, and SNEDDS.

Characteristic	SEDDS	SMEDDS	SNEDDS
Particle size	>300nm	<250nm	<100nm
Visual Appearance	Turbid	Clear	Clear
Surfactant HLB Value	<12	>12	>12
Lipid Formulation Classification system	Type II	Type IIIB	Type IIB
Oil Percentage	40-80%	<20%	<20%
Surfactant Percentage	30-40%	40-80%	40-80%

Nanoemulsions are kinetically stable while microemulsions are thermodynamically stable (21). This implies that for nanoemulsion, the free energy of the droplets in water is greater than the free energy of the separate phases while the reverse is the case for microemulsions (22). While the order of mixing will affect nano-emulsions, it does not affect microemulsions. Surfactants lower the interfacial tension and this aids dispersion processing. A co-solvent further aids the emulsification. Non-ionic surfactants with an HLB value greater than 12 are more desirable for SMEDDS as they are not as toxic as ionic surfactants (14).

1.3. Applications of SMEDDS and Current Drugs on Market

SMEDDS have great applications in the pharmaceutical industry and there are SMEDDS drugs currently on the market. Examples of drug currently on the market include Fenofibrate, Finasteride with a droplet size of 22.01–165.7nm, Berberine Hydrochloride

with a droplet size of 23.07nm, Andrographolide with a droplet size of 23.4±0.2 nm, Vinpocetine with a droplet size less than 50nm, Leuprorelin with a droplet size of 50.1nm (23). There are numerous ongoing research projects to develop essential oils as SMEDDS.

1.4. Release Profile of SMEDDS

Naturally, the presence of lipids in the duodenum stimulates the release of cholesterol and bile salts and form micelles. The hydrophilic part of the micelle is attracted to the aqueous side while the lipophilic part stays at the core as shown in figure 1.3.

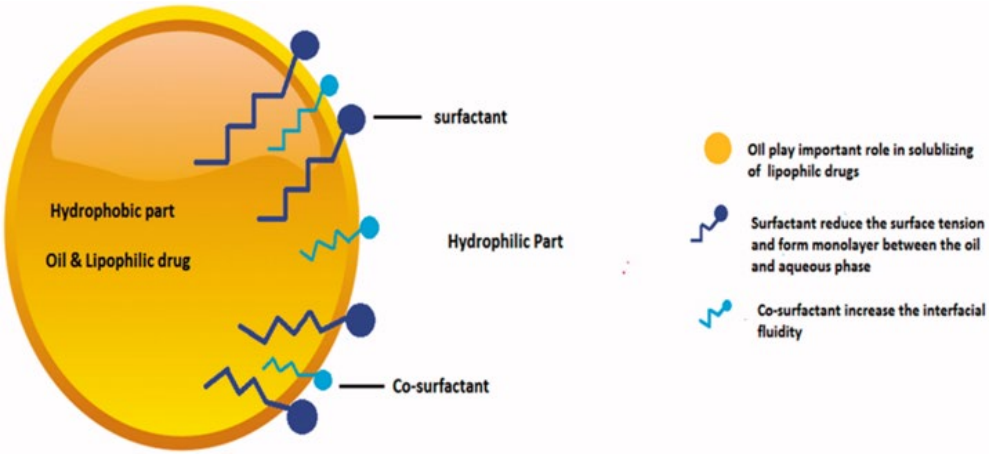

Figure 1-3. Structure of a SMEDDS (23).

Micellar solubilization is said to occur when a lipid formulation gets to the duodenum (24). This then causes the drug to be entrapped in a colloidal micelle and aids drug solubility. Also, SMEDDS can bypass hepatic degradation and go through lymphatic transport to the systemic circulation after being processed by intestinal lymph as shown in figure 1.4. The fate of solid-SMEDDS is comparable to liquid SMEDDS with little or no pharmacokinetic differences(25) (23).

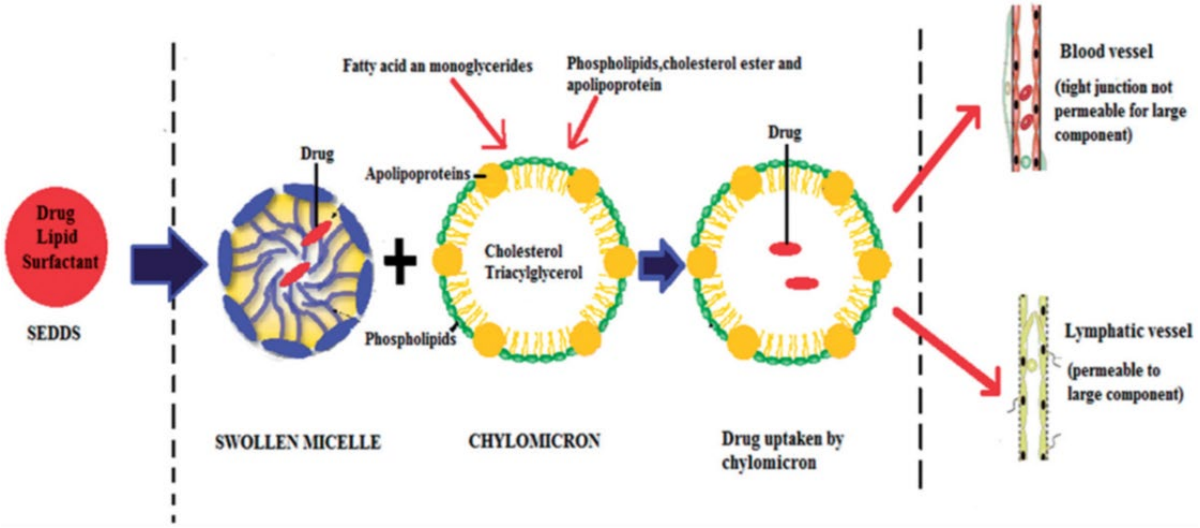

Figure 1-4. Route of Drug Through the Lymphatic System(23).

1.5. Challenges with SMEDDS

Dynamic light scattering (DLS) can be used to determine the mean droplet size of the emulsion but must be diluted before the measurement is taken. Dilution does not affect nano-emulsions, but it has been observed that micelles become swollen for micro-emulsions, and in a way, the measurement becomes does not fully represent the true mean droplet size (14). Precipitation of some SMEDDS upon dilution in the gastrointestinal tract is another limitation that has been reported in the literature. The incompatibility of some capsule shells with liquid-SMEDDS on long-term storage is another undesirable limitation. Some liquid-SMEDDS have been reported to be get absorbed into the capsule shell and interact with those capsules' shells over time. Solid-SMEDDS have been proposed to be a solution to these challenges. Also, This study is novel because it is one of the few studies on essential oils as solid-SMEDDS and it involves a further step of manufacturing various types of tablets from the solid-SMEDDS (26).

Chapter 2

Aim of Research

The objective of this study was to extract essential oil from the seeds of *Monodora myristica* and formulate the oil into a tablet that can form in-situ nanostructured dispersions. Fusion pro software was used for design of experiment to generate various possible formulation ratios of liquid-SMEDDS and to predict the best formulation ratio of liquid-SMEDDS to work with. The liquid-SMEDDS was adsorbed onto Neusilin US2 and different tablets were directly compressed using a tablet machine. The different tablets were characterized to determine the best formulation variables by performing thickness measurement, disintegration test, friability test, breaking force test, and drug content analysis. Fourier transfer infrared spectroscopy, scanning electron microscopy and differential scanning calorimetry were also performed on MMEO, liquid-SMEDDS, solid-SMEEDS, and the different types of tablets to physically characterize them.

Chapter 3

Materials and Methods

3.1 Materials

3.1.1 *Monodora myristica*

The peeled seeds of *Monodora myristica* were purchased from Carry Go Market (Missouri City, Texas). The seeds were identified by comparing them to catalog from the United States Department of Agriculture, Natural Resources Conservative Sciences. The seeds were blended and stored in airtight containers away from light at room temperature of 25℃.

3.1.2 Solid Adsorbance

Neusilin US2 was donated by Fuji Chemical Industries (Burlington, NJ). It is a unique form of amorphous magnesium aluminometasilicate. Large surface area and high oil adsorbing capacity are some of its properties. It is made up of white granules with a specific gravity of 2.0. The average particle size is 106 μm with an oil adsorbing capacity of 2.7-3.4 ml/g. It has a pH value of 7.4. It is insoluble in water but soluble in gastric acid.

3.1.3 Reagents

Transcutol HP and Labrasol were donated by Gatteffose Corporation (Paramus, NJ). Tween 80 was purchased from Fisher Chemical (Hampton, NH). Microcrystalline cellulose

pH 101 was purchased from FMC Corporation (Philadelphia, PA). Spray-dried lactose was purchased from Foremost Food Co. (Pomona, CA). Starch was purchased from Sigma Aldrich (St Loius. Mo). Talc was purchased from Letco Medical (Decatur, Al). Magnesium stearate was purchased from Fisher Scientific (Waltham, MA). Deionized water was obtained from the University of Toledo Health Science Campus. All solvents and reagents used were of analytical grade.

3.2 Methods.

3.2.1 Extraction and physicochemical characterization of the oil

Essential oil (MMEO) was extracted in batches from 3.2g of blended seeds by hydro distillation process using the Clevenger apparatus setup. The power regulator was kept at a temperature of 50 °C. Extraction from each batch was done for 4 hours. The MMEO was collected and separated from water by using a separatory funnel. It was then kept in glass containers and kept in the refrigerator away from light.

3.2.2 Physiochemical Characterization of MMEO

The following properties were determined for MMEO, percentage yield value, color, solubility in alcohol, density, specific gravity, refractive index, viscosity, saponification value, iodine value, acid value, peroxide value, and free fatty acid value. All the physicochemical characterization was done using Guenther (1952) (27) and AOAC (2000) (27) methods.

3.2.2.1 Yield Value

3.89g of the seed was used in the extraction process. The percentage yield value was calculated using the formula:

Yield value (%) = (weight of oil ÷ weight of sample) × 100%.---------Eqn. (3.1)

3.2.2.2 Color Determination

The color of MMEO was examined by visual observation.

3.2.2.3 Solubility in Alcohol

The solubility of MMEO was determined by using a calibrated pipette to add drops of ethanol to 1ml of the essential oil at 25°C. The mixture was shaken thoroughly after each drop of ethanol and the color was observed. The addition of ethanol was stopped when a clear solution was obtained. This is according to Guenther's method.

3.2.2.4. Density

Density determination of MMEO was done using a pycnometer at a temperature of 25℃. The pycnometer was initially washed with ethanol and thereafter rinsed with ether. The pycnometer was dried in the oven and then weighed. It was filled with deionized water, closed with its lid, and kept in a water bath for about 30 minutes. This was done to ensure that the pycnometer and the water stabilized to the temperature of the water bath; 25℃. The pycnometer was then reweighed. This procedure was repeated using MMEO. The whole procedure was done in triplicates and the average values and standard deviations were reported. The density of MMEO was done using the following equation:

The volume of pycnometer = ((Mass of water-Mass of air)/(Density of water-Density of air)) ----------Eqn. (3.2)

The density of MMEO= ((Msample-Mair)/ Volume) + Density of air))……..Eqn. (3.3)

Specific gravity= (Density of MMEO) / (Density of water)----------Eqn. (3.4).

3.2.2.5. Refractive Index

Rudolph's J257 automatic refractometer (Rudolph Research Analytical, NJ, USA) was used to determine the refractive index of MMEO. The prism was cleaned with acetone and afterward calibrated with water. The Refractive index of both water and MMEO were measured at temperatures 20℃ and 25℃. Readings were done in triplicates. The average value and standard value were reported.

3.2.2.6. pH Value.

MMEO pH was determined using the Metler Toledo Seven Multi pH meter. pH buffer 7, 4, and 10 were used to calibrate the instrument. Readings were done in triplicates at a temperature of 25℃.

3.2.2.7. Viscosity.

Essential oil's viscosity can be determined using an Ostwald viscometer. The viscometer was properly cleaned and dried. The viscometer was put in a standing position by clamping it in a vertical position. About 3ml of the sample was pipetted into tube A and suction was applied to tube B until the upper level of the sample is above mark C. A stopwatch was then used to measure the time it took for the sample to move from marks C and D. This procedure was done for deionized water and MMEO. Readings were done in triplicates.

The average value and standard value were reported. The viscosity of MMEO was calculated using the following equation:

η_2= ((ρ2t2)/(ρ1t1) / (ρ1t1)× η_1----------Eqn. (3.5)

Where η_1=absolute viscosity of water, η_2=absolute viscosity of MMEO, $t1 =$ time of flow of water, $t2 =$ time of flow of MMEO, $\rho 1 =$ density of water and ρ2=density of MMEO.

3. 2.2.8. Saponification Value (SV).

This is a measure of how much alkali is needed for the complete saponification of all the triglycerides present in MMEO. 25ml of alcoholic potassium hydroxide (K(OH)4) was added to a conical flask containing 2g of MMEO. A reflux condenser was then attached to the conical flask and the mixture was heated for 1 hour with constant shaking. After which one milliliter (1 ml) of 1 percent phenolphthalein indicator was added to the mixture and 0.5M hydrochloric acid (HCl) was titrated against the remaining alkali until it turned colorless. The endpoint is the point at which the mixture turns colorless. A blank titration was done using the same method. Readings were done in triplicates and the average SV and standard deviation were reported. SV was determined using this equation:

Saponification value= (Mw ×N× Vblank -Vtest)/ Ws----------Eqn. (3.6).

Where: Mw=molecular weight of KOH(g/mol), Vblank= vol of HCl for blank sample(ml), Vtest=vol of HCL for the test sample, N= normality of HCL (mol/ml) and Ws= sample weight.

3.2.2.9. Acid Value (AV)

The amount of potassium hydroxide (KOH) needed to neutralize the free oil in 1g of the sample indicates the acid value. This was done by neutralizing a mixture of 25ml of diethyl-ether, 25ml of ethanol, and 1ml of 1% phenolphthalein indicator with 0.1M sodium hydroxide (NaOH) solution. 1gram of MMEO was dissolved in the total mixture and titrated with aqueous 0.1M NaOH. A pink color that lasted for about 15 seconds indicated the endpoint and the titration were done with constant shaking. The procedure was done in triplicates and both the average titer and standard deviation were recorded. The acid value was calculated with the equation:

$$\text{Acid value} = (V \times M \times 40)/ \text{ weight of sample} \quad \text{----------Eqn. (3.6)}$$

where, v = Volume of NaOH used for titration and M = Molarity of NaOH used.

3.2.2.10. Free Fatty Acid Value (FFAV)

The free fatty acid value was determined by the formula:

$$\text{Free fatty acid} = \text{acid value}/ 2 \quad \text{----------Eqn. (3.7)}$$

This was done in triplicate and the average and standard deviation were reported.

3.2.3. Design of Experiment of Self-Micro emulsifying Lipid Formulations (SMEDDSs)

Liquid-SMEDDs were conceptualized by the design of the experiment (28) by combining MMEO, a surfactant, and a co-surfactant. The first combination (A) included MMEO, Tween 80 (surfactant), and Transcutol HP (co-surfactant) while the second combination (F) included MMEO, Kollipor (surfactant), and Labrasol (co-surfactant). “The goal for class IIIB was that the oil phase should be less than 20%, the hydrophilic surfactant (HLB>

12) should be between the range of 20-50% while the co-surfactant should be between the range of 20-50%"; according to (Pouton 2000) lipid formulation classification(29). 7 different ratios of both A (A3, A6, A9, A10, A12, A13, A15) and F(F3, F6, F9, F10, F12, F13, F15) formulations were studied by using Fusion Pro by S-Matrix (Fusion Pro Software Version 9.9.0 Build 690, S-Matrix Corporation (www.smatrix.com)) to predict the best self-emulsifying region. The mixture variables were (MMEO, Tween 80, Transcutol HP, Labrasol, and Kolliphor) while the process variables were their varied weight percentages. Statistical analysis was also performed using Fusion Pro software .

3.2.4. Liquid-SMEDDS Formulations.

MMEO, surfactants, and co-surfactants were prepared by a vortex machine for 20 minutes. 500mg of each formulation (A and F formulation ranges) were prepared with varying weight percentages.

3.2.5. Liquid-SMEDDSs Optimization

Characterization was done for the 14 formulations and the values were inputted into the Fusion Pro software to predict the best mixture variable. Emulsification was achieved by titrating all the 14 formulations with DI water (1ml:100ml). The mixture was then homogenously mixed using a vortex mixer for 20 minutes individually. Emulsification time in seconds was obtained by noting the time it took for emulsions to be properly formed. Visual appearance was done by physical observation. The formulations were covered and stored at 25°C for 60 days. Stability in days was also studied over this time range. The mean particle size and zeta potential of all the formulations were also determined by using PSS.NICOMP Particle sizing systems; Saint Barbara, CA, USA.

Analysis was done by using Fusion Pro by S-Matrix (Fusion Pro Software Version 9.9.0 Build690, S-Matrix Corporation (www.smatrix.com)) to predict the best ratio of the ingredients to work with.

3.2.6. Final Liquid-SMEDDS Formulation and Characterization

Based on the quality by design optimization done, 10.92% of MMEO was initially mixed with 48% of Tween 80 with a vortex mixer for about ten minutes. 41.08% of Transcutol HP was then added to the mixture and then mixed for another 10 minutes using a vortex mixer. 500 mg of the formulation was diluted with 50 ml of water in a volumetric flask under stirring conditions. The particle size and the zeta potential were determined using PSS NICOMP TM 380 ZLS; Saint Barbara, CA, USA. Three batches of 500 mg of the formulation were subjected to heating and cooling cycles, by cooling at 4 °C for 24 hours followed by heating at 40 °C for 24 hours. After this, they were diluted with 50 ml of DI water and the emulsion was studied.

3.2.7. Preparation of Solid-SMEDDS and Characterization

3.2.7.1 Preparation of Solid-SMEDDS.

Solid-SMEDDS was prepared by absorbing optimized liquid-SMEDS into neusilin US2. The neusilin US2 was gradually added into a mortar containing the liquid-SMEDDS with constant mixing using a pestle. This was continuously done until a homogenous powder with good flowability was obtained. The adsorption capacity was also determined by using the equation:

Adsorption capacity (AC)= (Weight of L-SMEDDS (g)) / (Weight of Solid Carrier (g))----------Eqn. (3.8).

3.2.7.2. Solid -SMEDDS In-Vitro Characterization.

Solid-SMEDDS (0.1g) was dispersed in 100ml of DI water and vortexed for 10 minutes. The solution was filtered, and a clear emulsion was gotten. The size of the dispersed droplets was determined using a PSS NICOMP TM 380 ZLS; Saint Barbara, CA, USA**.** Solid-SMEDDS was further characterized by determining the true density, bulk density, tapped density, Carr index, Hausner ratio, and porosity.

The true density was determined using a pycnometer. The initial weight of an empty pycnometer was initially determined. The bottle was then filled with water and reweighed. The water was removed, and the pycnometer was dried. Solid-SMEDDS was added to the pycnometer and reweighed. DI water was added to the solid-SMEDDS in the pycnometer and weighed again. Measurements with the pycnometer were done with a close-fitting ground glass stopper. The true density was then determined using the formula:

True Density= $[[c - a]] \times 1g/cm3 \div$ [[b-a]-[d-c]]----------Eqn. (3.9).

Where a is the weight of the empty bottle, c is the weight of the empty bottle + powder, d is the weight of bottle +water + powder, b is the weight of bottle +water.

The bulk density was determined by using the formula:

Bulk Density= Weight of powder/ bulk volume of powder----------Eqn. (3.10).

The tapped density was determined using the formula:

Tapped density = Weight of Powder/ tapped volume of powder----------Eqn. (3.11).

The Carr Index was determined using the formula:

Carr Index= [tapped density-bulk density]/ tapped density. ---------Eqn. (3.12).

The Hausner's ratio was determined using the formula:

Hausner's ratio= tapped density/bulk density----------Eqn. (3.13)

The porosity was determined using the formula:

Porosity= 1- [bulk density/ true density] * 100%

All readings were taken in triplicates, the means and standard deviation were reported.

3.2.8. Tablet Compression and Characterization

3.2.8.1. Tablet Compression.

All ingredients needed for tablet compression were accurately weighed. The materials and the percentages used for the different types of tablets can be seen in table.3.1. The ingredients such as solid-SMEDDS, cellulose, lactose, starch, talc, and magnesium stearate served as an active pharmaceutical ingredient, binder, diluent, diluent, glidant, and lubricant respectively. Solid-SMEDDS, microcrystalline cellulose, lactose, and starch were individually sieved using sieve no. 40 except talc and magnesium that were individually sieved through sieve no.80. Powder mixtures were then blended for ten minutes using a

Shaker Mixer TURBULA® Type T2 C; Switerzland to obtain uniform mixtures. Sieving the powders was done to remove powder agglomerates that can prevent excellent compression of the powder mixtures while blending the powder mixtures was done to ensure uniformity of the ingredients in the compressed tablets.

Table 3. 1. Percentage Composition for Type 1, 2, and 3 Tablets.

Ingredient	Pharmaceutical Use	TYPE 1(%)	TYPE 2(%)	TYPE 3(%)	BLANK (%)	BLANK (%) TYPE 3
Solid-SMEDDS	API	25	28	45	25	45
Microcrystalline cellulose	Binder	29	38	55	29	55
Spray Dried Lactose	Diluent	32	20		32	
Starch	Diluent	10	10		10	
Talc	Glidant	3	3		3	
Magnesium stearate	Lubricant	1	1		1	

The angle of repose was determined for the powder used to manufacture type 1, type 2, and type 3 tablets. A funnel was attached to a tripod stand with a paper spread on the base to receive the powder. The height of the funnel was kept at 2cm to 4cm to build a symmetrical cone of powder. The vibration was eliminated to prevent disturbance. The height and radius of the powder were recorded, and the angle of repose was determined using the formula below:

$$\text{The angle of repose} = \arctan(h/r) \quad \text{----------Eqn. (3.14)}$$

Where h is the height of the heap in cm and r is the radius in cm.

Different types (Type 1, type 2. Type 3, Blanks) of tablets were produced by direct compression using a flat round standard 0.375-inch tooling and flat punch and die set. The direct compression used was the single station tablet press machine (Emil Korsh Maschinen Fabrik, Berlin, Germany). The tablet weight (die volume) was kept at 200mg and the compression force was also kept constant.

3.2.8.2. Tablet Characterization

3.2.8.2.1. Tablet Weight variation

Tablet weight variation was determined by weighing 20 individual tablets for each type and reporting the weight and standard deviation.

3.2.8.2.2. Tablet Thickness Test

Tablet thickness was determined for the three sets for each type of tablet using a Vinca Dcla-0605 Electronic Digital Vernier Micrometer Caliper.

3.2.8.2.3. Tablet Friability

Tablet Friability was done in a Roche friabilator (Erweka, Germany). Around 6.5g of each table type was weighed and placed in the friabilator. 25rpm was set as the rotation speed for 4 minutes. The tablets were re-weighed. Percentage friability was set calculated using the equation:

$$\%\ friability = (WI - WF)/WI \times 100\% \quad \text{Eqn. (3.9)}$$

where WI and WF are initial and final tablet weights, respectively. Readings were taken in triplicates and the standard deviation was reported.

3.2.8.2.3. Tablet breaking force

The breaking force was manually done using a manual hardness tester (US patent no 2041869) and a digital electronic breaking force (type H1 T, Sotax, MA, USA). Six sets of tablets per tablet type were used for each breaking force test.

3.2.8.2.4. Tablet Disintegration Test

Tablet disintegration test was performed in a USP Tablet Disintegration apparatus. Six sets of tablets for each tablet type were used to determine the time it took for the tablets to disintegrate. In-vitro disintegration test was done as per USP requirements for immediate release tablets. Six tablets were put in each tube of the disintegration apparatus (Erweka, Germany) and immersed in DI water at a temperature of 37±1ºC. The time it took for the tablets to disintegrate was recorded. Times for complete disintegration of each of the tablets were recorded. The studies were done in triplicate and the average value and standard deviation were reported.

One-way ANOVA was used to statistically determine if there was a difference between the tablet thickness, breaking force, disintegration time, and friability.

3.2.9. Drug Content Analysis

3.2.9.1. Calibration Curve

To determine the wavelength maxima for MMEO, the wavelength between 240nm to 400nm with the highest absorbance was observed. A calibration curve was generated by initially diluting a 100mg/mL stock solution to concentrations of 31.25, 15.625, 7.1825, and 3.90625 mg/mL with methanol. Equation C1V1=C2V2 was used to calculate the total volume of dilution. Constant mixing using a vortex mixer for about 5 minutes was done

for each of the samples. The solutions were then placed in clean cuvettes with clear sides facing the laser. The absorbance was then measured at 243 nm using Genesys 10S UV-VIS spectrophotometer (Thermo Scientific, MA, USA).

3.3.9.2. Drug Content of Type 1, Type 2, and Type 3 Formulations

Three tablets per tablet type were weighed and crushed in a ceramic mortar. They were individually mixed with 4ml of methanol each using a vortex mixer. The solutions were filtered through a 0.20 μm membrane filter (EMD Millipore®, Fisher Scientific) and absorbance was measured at 243nm using a Genesys 10S UV-VIS spectrophotometer (Thermo Scientific, MA, USA). Blank tablet filtrates were used as the blank for absorbance measurements. The studies were done in triplicate and average values and standard deviations were reported. In general, drug content analysis was done over three weeks to see what happens to the tablets over time.

3.2.10. Fourier Transform IR Spectroscopy (FTIR).

Fourier transform infrared (FTIR) spectroscopic analysis of MMEO and its emulsion was performed using Thermo Scientific Nicolet iS5 (MA, USA) and potassium bromide pellet method. The resolution was maintained at 4 cm−1 and a range of 400–4000 cm−1. Background spectra were collected before each sample measurement

3.2.11. Differential Scanning Calorimetry (DSC)

For DSC analysis, 9.9 mg of MMEO, 9.8mg of liquid-SMEDDS, 9.4mg of solid-SMEDDS, 5.6mg of neusilin US2 were used. The samples were crimped into 40 μl aluminum pans and sealed with aluminum lids. A heating rate of 5°C/min with a continuous flow of nitrogen gas of (40 mL/min) was employed. The heating cycle was −40 to 120 °C

for both MMEO and liquid-SMEDDS while -40 till 300°C for both the solid-SMEDDS and neusilin US2 using TA Instruments Q20 DSC (UT, USA).

3.2.12. Scanning Electron Microscopy (SEM)

Morphology of the emulsion was done using Scanning electron microscopy (JEOL JSM-7500F USA) with a Transmission Electron Detector. Before the analysis, the liquid-SMEDDS sample was diluted with 100ml of DI water to form an emulsion, placed on 400-mesh copper grids with and left to dry. The surface structure of neusiln US2, solid-SMEDDS, type 1 tablet, type 2 tablet, and type 3 tablet were done using Scanning electron microscopy (JEOL JSM-7500F USA) full mode. All the samples were gold-coated before analysis using Denton Desk II Sputter Coater (USA).

Chapter 4

Results and Discussion

4.1. Physiochemical Characterization of MMEO.

The yield value of MMEO was derived to be 2.53% w/w. This was similar to the yield value; 2.46 %w/w and 4.36%w/w reported by Rahardiyan et.al (30). Plant origin and period of the collection have been observed to affect yield variation. MMEO's color was observed to be lightly golden and this was similar to the color reported by Ekere et.al (28). 1 part of MMEO is soluble in 1 part of ethanol and insoluble with DI water. The density and specific gravity of MMEO were observed to be 0.855 ±0.03 g/ml and 0.858 ±0.00 g/ml respectively. Specific gravity can be defined as density divided by the density of water. MMEO specific gravity is less than 1. Specific gravity can be used to predict the purity of a sample and it was within the range (0.82-0.92) reported in the literature (31). The refractive index can be described as the ratio of the speed of light in a vacuum relative to the oil. It gives an idea of the intensity of double bonds and the degree of unsaturation in a sample. Oxidative damage can be deduced from this information. The Refractive index of MMEO was found to be 1.479 ± 0.00 and 1.477 ± 0.00 at 20℃ and 25℃ respectively. The refractive index was comparable with the one reported by Akise et.al (31).

The viscosity of MMEO is 0.52 ± 0.001 cP which indicates that it is less viscous than water (0.89 cP) at 25℃. The pH of MMEO was found to be 5.151 indicating that the essential oil was slightly acidic. MMEO had a saponification value (SV) of 183.4 ±1.14 mg KOH/g and it can be compared with the SV; 185.13 mg KOH/g reported by Aise et.al. SV can be used to measure the fraction of low molecular weight triacylglycerols in oil samples. The higher the SV, the higher the number of ester bonds and the average molecular weight of fatty acids in an oil sample. Also, there exists an inverse proportionality between the SV and the chain length of fatty acids in fats and oils. The essential oil derived from *Piper guineense* was reported to have a longer fatty acid chain length compared to MMEO(31). The acid value (AV) 6.13 ± 0.03 mg KOH/g was about the same (6.73 mg KOH/g) reported by the Aise et.al. Free Fatty Acids (FFA) of essential oil can be deduced from the acid value (AV). The higher the AV, the lower the edibility of the oil. A value less than 10mg KOH/g was found to be suitable for dietary purposes. Essential oils with lower AV have also been described to have higher stability and fewer chances of becoming rancid with time. The physicochemical properties of MMEO indicate that the oil is of good pharmaceutical value.

Table 4. 1. Physiochemical Characteristics of MMEO.

Physiochemical Characteristics	Value
Yield value	2.53%w/w
Color	Light gold
Solubility in ethanol	1:1 soluble
Density	0.855 ±0.03 g/ml
Specific gravity	0.858 ± 0.004
Refractive Index at 20℃.	1.4790 ± 0.00
Refractive index at 25℃.	1.4766 ± 0.00

pH	5.151 ± 0.004
Viscosity	0.52 ± 0.001cP
Saponification Value	183.4 ± 1.14 mg KOH/g
Acid Value	6.13 ± 0.03 mg KOH/g

4.2 Design of Experiment (28) of Liquid-SMEDSs.

A DOE is a very instrumental experimental design that can accommodate all possible variables and statically predict the best possible conclusion(32). DOE has been established to be very effective in a systematic way. 15 formulations were created by the DOE with 12 of them being unique formulations while 3 of them were duplicates to address the noise within Fusion Pro's analysis software. The formulations can be seen in table 4.2. 7 different ratios of each combination were chosen since MMEO should be between 1% to 20%, the surfactant should be between 20% to 50% and the co-surfactant should also be between 20% to 50%.

Table 4. 2. A and F L-SMEDDS Formulations

Name: eagbolu@outlook.com
Company: University of Toledo
Project: SMEDDSs
Date: 16 OCT 2020 12:12:39 EDT [UTC-04:00]

Experiment Design - Experiment 1

Experiment Constants

Constant Name	Constant Value	Units
Mixture Amount	100.00	%

Experiment Design Matrix

Run No.	OIL (%)	SURFAC TANT (%)	CO-SURFAC TANT (%)
1	10.50	39.50	50.00
2	1.00	49.50	49.50
3	20.00	50.00	30.00
4	20.00	30.00	50.00
5	1.00	49.00	50.00
6	15.25	37.38	47.37
7	1.00	50.00	49.00
8	20.00	50.00	30.00
9	10.50	44.75	44.75
10	5.75	47.38	46.87
11	20.00	30.00	50.00
12	20.00	40.00	40.00
13	15.25	47.38	37.37
14	10.50	44.75	44.75
15	10.50	50.00	39.50

4.3. Liquid-SMEDDS Formulation

The amount of each ingredient used in the formulations is shown in Tables 4.3 and 4.4.

Table 4. 3. Percentage Composition of A Liquid-SMEDSS Formulations.

FORMULATION	MMEO [%}	TWEEN 80 [%]	TRANSCUTOL [%]
A3	20	50	30
A6	15.25	37.38	47.37
A9	10.50	44.75	44.75
A10	5.75	47.38	46.87
A12	20	40	40
A13	15.25	47.38	37.37
A15	10.50	50	39.50

Table 4. 4. Percentage Composition of F Liquid-SMEDDS Formulations.

FORMULATION	MMEO [%}	KOLLIPHOR [%]	LABRASOL [%]
F3	20	50	30
F6	15.25	37.38	47.37
F9	10.50	44.75	44.75
F10	5.75	47.38	46.87
F12	20	40	40
F13	15.25	47.38	37.37
F15	10.50	50	39.50

4.4. Liquid-SMEDDS Optimization

Emulsion characterization can be seen in table 4.5, 4.6, and 4.7. Formulation A2 had the lowest emulsification time (22 seconds) while formulation A13 had the largest emulsification time (65seconds). Emulsification was achieved under less than 2 minutes for all the formulations and this indicates that the liquid-SMEDDS can spontaneously form emulsions in the gastrointestinal tract which is a precursor to drug solubility and absorption into the gastric lumen. All the A formulations did not exhibit flocculation while F formulations exhibited flocculation which was consistent over 60 days. The presence of flocculation indicates emulsion instability. Turbidity was determined on a scale of 1-10 where 1 was compared to the visibility of water by visual observation. Formulations A15 and F10 had the same visual appearance as water while Formulation F13 had the highest turbidity. All the formulations had visibility of less than 6. For type A formulations, the visibility was seen to get clearer over five days while flocculation was seen to increase for all type F formulations except for F10 and F15. The stability determined by zeta potential analysis for the emulsion was not a concern since the emulsions formed will exist for few hours in the gastrointestinal tract. Formulation F3 had the highest particle size (218 nm) while A10 had the lowest particle size (12.3 nm). Lower particle size is desirable as this

greatly affects the rate and extent of MMEO absorption. The polydispersity was less than 1 which reflects the emulsions are isotropic except for A3 that had a PI of 0.8 and is more polydisperse than the others.

Table 4. 5. A Pre-formulation Studies

FORMULATION	MMEO [MG]	TWEEN 80 [MG]	TRANSCUTOL[MG]	EMULSIFICATION TIME[SECS]	STABILITY 1ST DAY	STABILITY 2ND DAY	STABILITY 3RD DAY	STABILITY 4TH DAY	STABILITY 5TH DAY
A3	100	250	150	30	Less Turbidity-4	3	2	2	1
A6	76.3	186.9	236.9	22	Less turbid-4	3	3	3	3
A9	52.5	223.8	223.8	41	Clear-2	Clear-2	Clear-1	Clear-1	Clear-1
A10	28.8	236.9	234.4	60	Clear -2	Clear 1	Clear 1	Clear 1	Clear 1
A12	100	200	200	45	Less turbid-4	2	2	2	2
A13	76.3	236.9	186.9	65	Less turbid-4	3	3	2	2
A15	52.5	250	197.5	42	Clear-1	Clear-1	Clear-1	Clear-1	Clear-1

Table 4. 6. F Pre-formulation Studies

FORMULATION	MMEO [MG]	KOLLIPHOR[MG]	LABRASOL[MG]	EMULSIFICATION TIIME[SECS]	STABILITY 1ST DAY	STABILITY 2ND DAY	STABILITY 3RD DAY	STABILITY 4TH DAY	STABILITY 5TH DAY
F3	100	250	150	60	Slightly Turbid-5	Less Turbid-5. Few particles	Less turbid-5. Few particles	Less turbid-5. More particles	Less turbid-5. More particles
F6	76.3	186.9	236.6	50	Transparent- 2. No particles	Transparent-2. No particles	Transparent- 2. No particles	Transparent – 2. 1 to 2 particles	Transparent- 2. 1 to 2 particles

F9	52.5	223.8	223.8	62	Slightly Turbid-4.	A bit turbid-3. 1 to 2 particles	A bit turbid-3. 1 to 2 particles	A bit turbid. 1 to 2 particles	A bit turbid. Few particles
F10	28.8	236.9	234.4	53	Clear-1.	Clear 1. Few particles	Clear 1. Few particles	Clear 1. Few particles	Clear 1. Few particles
F12	100	200	200	50	Transparent- 2	Clear 1. 1 to 2 particles	Clear 1. 1 to 2 particles	Clear 1. 1 to 2 particles	Clear 1. Few particles
F13	76.3	236.9	186.9	60	Slightly turbid-5	Turbid-5. A lot of particles	Turbid-5. A lot of particles	Less turbid-4. More particles	Less turbid -4. More particles
F15	52.5	250	197.5	57	Transparent-2	Clear-1. 1 to 2 particles	Clear-1. 1 to 2 particles	Clear-1. 1 to 2 particles	Clear-1. 1 to 2 particles

Table 4. 7.Mean Particle size, Polydispersity, and Zeta Potential of A and F Batches

Formulation	Mean Particle Size [nm]	Polydispersity	Zeta Potential [mv]
A3	162.4	0.8	-1.10
A6	41	0.1	105.8
A9	183.8	0.2	-0.91
A10	12.3	0.1	-89.4
A12	38.5	0.2	98.5
A13	105.9	0.6	3.8
A15	142	0.4	39.5
F3	218.3	0.1	-3.3
F6	23.7	0.4	-126.7
F9	16.5	0.02	0.03
F10	14.7	0.1	-141
F12	137.7	0.1	101.7
F13	18.6	0.1	0.02
F15	17.3	0.1	-52.2

Based on the characterization done, the Fusion Pro matrix did the prediction analysis to determine the best ratio of the ingredients to work with. The optimum performance region for type A formulation was MMEO (10.92%), Tween 80 (48%), and Transcutol HP (41.08%) as shown in figure 4.1. The predicted response value for emulsification time was 21.97 seconds, visual appearance was 2.27, mean particle size was 78.23 nm

Study Variable Data

Study Variable Name	Prediction Point Level Setting
MMEO	10.92
TWEEN 80	48.00
TRANSCUTOL	41.08

Predicted Response Data

Response Variable Name	Predicted Response Value	-2 Sigma Confidence Limit	+2 Sigma Confidence Limit
Emulsification time	21.9782	-6.4268	50.3833
Visual appearance	2.2780	-0.2959	4.8518
MEAN particle Size	78.2340	-161.9834	318.4515
Zeta potential	35.6212	-88.8703	160.1128

Experiment Constants

Constant Name	Constant Value	Units
Mixture Amount	100.00	%

Figure 4-1. Type A Best Overall Answer.

Type A acceptable performance region (APR) is shown in figure 4.2 with the overlay included. Beyond the APR, the desired emulsion characteristics are not achievable.

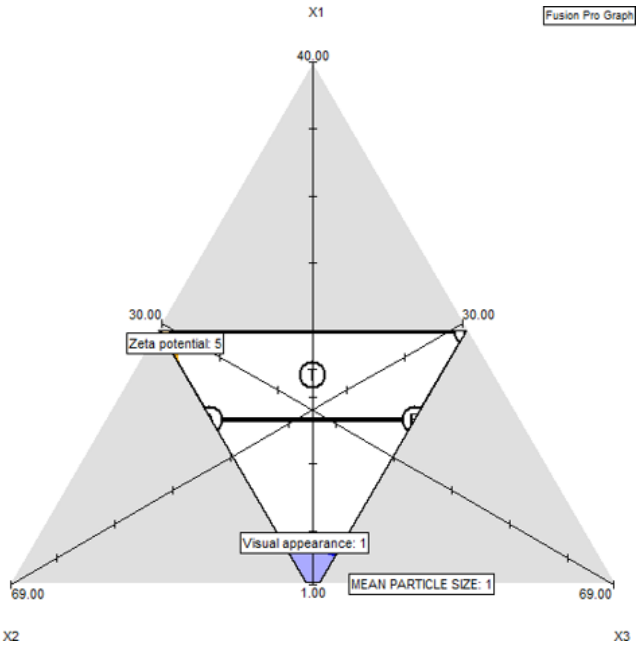

Figure 4-2. Type A Acceptable Performance Region.

The response trace plot is shown in Figures 4.3-4.5. It can be deduced that as the percentage of MMEO increases, co-surfactant increases and surfactant reduces, the visual appearances move from 1 to 10 on a turbidity scale and emulsification time increases. As the percentage of MMEO composition increases, the particle size increases.

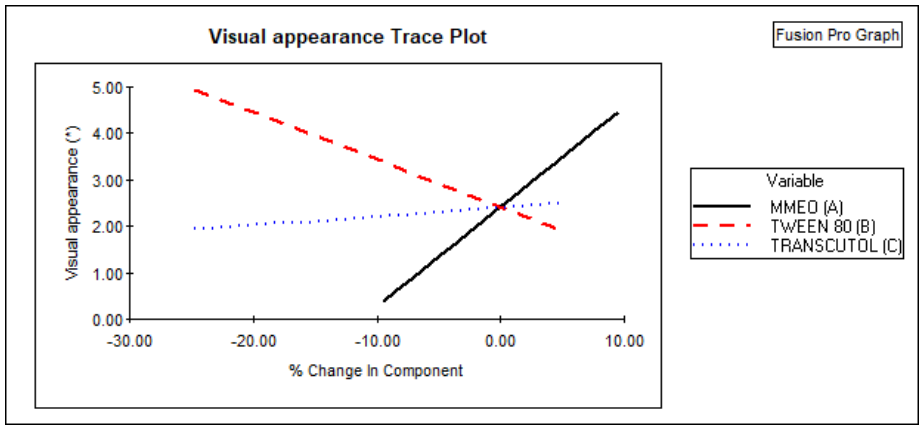

Figure 4-3. Visual Appearance Trace Plot

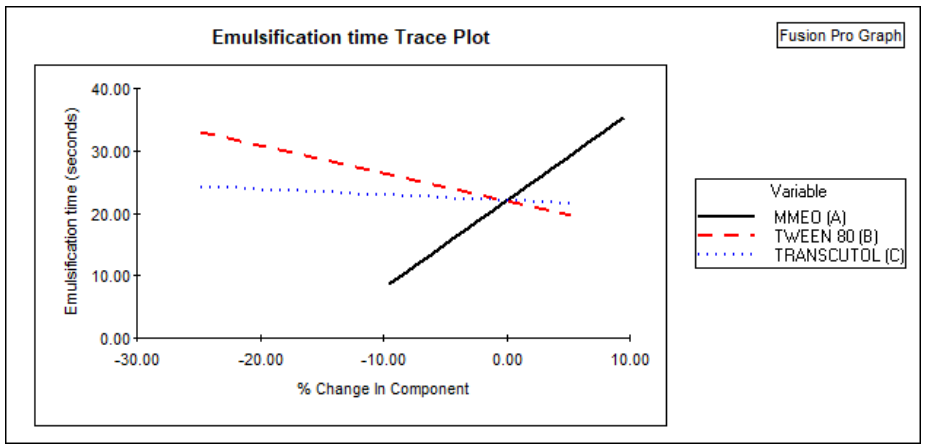

Figure 4-4. Emulsification Time Trace Plot

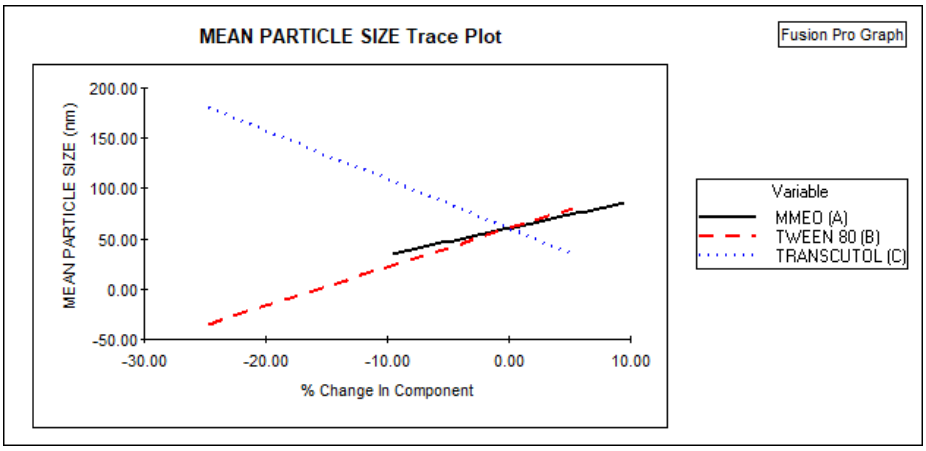

Figure 4-5. Mean Particle Size Trace Plot

Based on the characterization done, the fusion pro matrix did the prediction analysis to determine the best ratio of the ingredients to work with. The optimum performance region for type F formulation was MMEO (10.50%), Kolliphor was (39.50%) and Labrasol was (50%) as shown in figure 4.6. The predicted response value for emulsification time was 51.41 seconds, visual appearance was 1.37, mean particle size was 32.65 nm.

Study Variable Data

Study Variable Name	Prediction Point Level Setting
MMEO	10.50
SURFAC TANT	39.50
CO-SURFACTANT	50.00

Predicted Response Data

Response Variable Name	Predicted Response Value	-2 Sigma Confidence Limit	+2 Sigma Confidence Limit
Emulsification time	51.4067	36.3120	66.5013

Visual appearance	1.3718	-3.1222	5.8657
Particle size	32.65	-102.1161	170.57
Zeta potential	95.5809	-37.1999	228.3617

Experiment Constants

Constant Name	Constant Value	Units
Mixture Amount	100.00	%

Figure 4-6. Type F Best Overall Answer

Type F acceptable performance region (APR) is shown in figure 4.7 with the overlay included. Beyond the APR, the desired emulsion characteristics are not achievable.

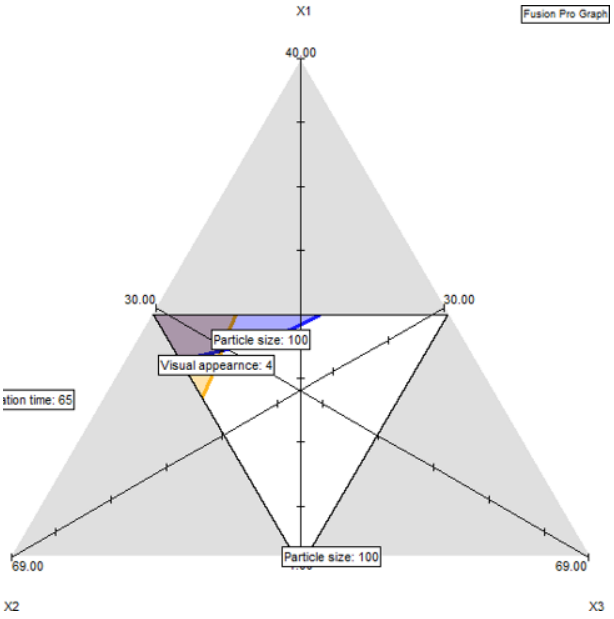

Figure 4-7. Type F Acceptable Performance Region

The response trace plot is shown in Figures 4.8 to 4.10. It can be deduced that as the percentage of MMEO increases, surfactant increases and co-surfactant reduces, the visual appearances move from 1 to 10 on a turbidity scale. As the percentage of MMEO and

Labrasol reduces, Kollipor increases, emulsification time increases. There is no direct relationship between the percentage change in the composition of (MMEO, Kollipor, Labrasol) and particle size.

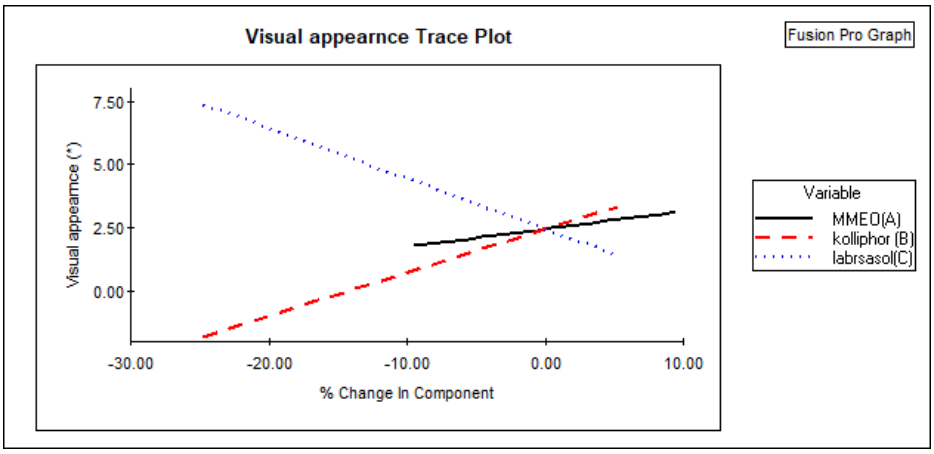

Figure 4-8. Visual Appearance Trace Plot

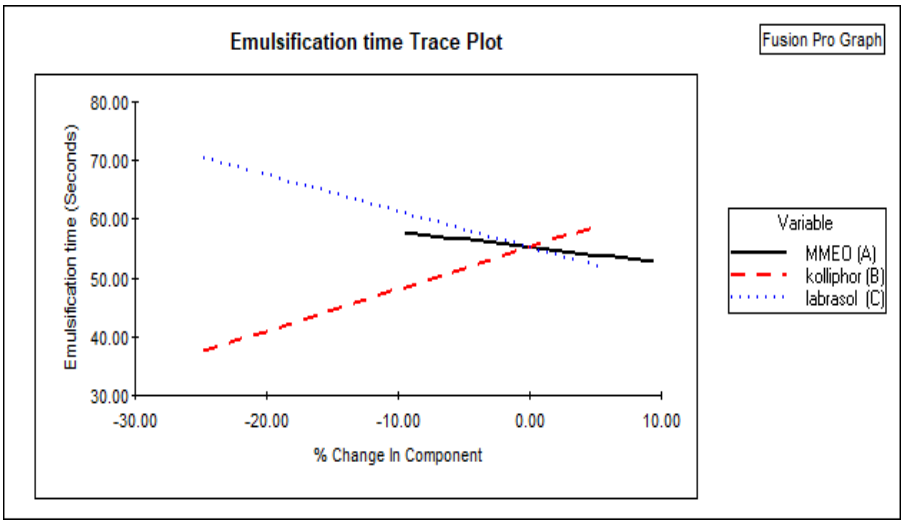

Figure 4-9. Emulsification Time Trace Plot

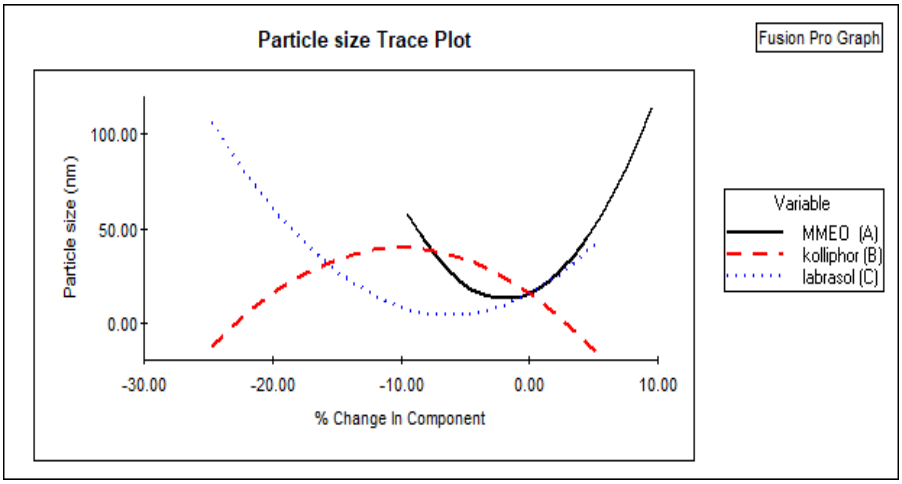

Figure 4-10. Particle Size Trace Plot

Tween 80 and Transcutol HP were chosen as the surfactant and co-surfactant in the final ingredients. Flocculation was observed with kolliphor and labrasol which persistently increased over 60 days and this was the reason why the combination was not pursued. Drug precipitation has been reported with some SMEDSS which is not a desirable characteristic. Also, type F prediction was not pursued because the percentage composition of surfactant should not be less than co-surfactant. The mean particle size predicted for type A is also within the acceptable goal. How stable an emulsion will be over days can be inferred from the zeta potential of the emulsion. The stability of the emulsion over days was not considered since the emulsion will be in the gastrointestinal tract for not more than 7hours.

4.5. Final Liquid-SMEDDS Formulation

For the thermodynamic stability study, no form of phase separation or coalescence was observed with thermodynamic stress as shown in figure.4-11. The mean particle size was

determined to be 112.7 nm as shown in figure.4.12 and it was over a wide range indicating there were different particle sizes in the emulsion. This was a bit above the particle size predicted by the DOE, but it was acceptable since microemulsions usually range from 100 nm to 250 nm. The zeta potential was determined to be +5.10mv as shown in figure.4.13. Positively charge microemulsions can penetrate the mucosal lining better than negatively charge microemulsions which have been reported to result in greater bioavailability(33).

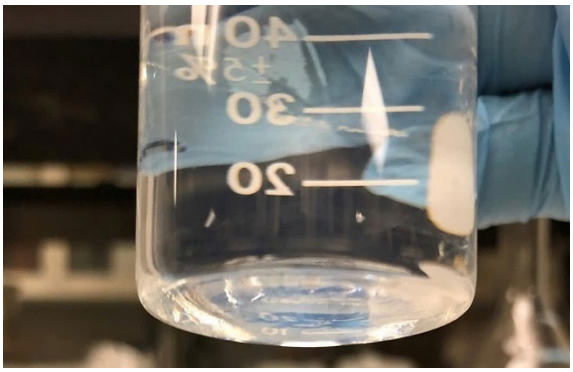

Figure.4-11. Picture of Emulsion Subjected to Thermodynamic Stress.

Particle Sizing Systems, Inc.
Santa Barbara, Calif., USA

OILTWEEN80KOLLIPHOR
Menu File: C:\Documents and Settings\PSSNicomp\Desktop\ELIZA\FINALFORM.OOO.tbl 15:4:40

INTENSITY-Weighted NICOMP DISTRIBUTION Analysis (Solid Particle)

NICOMP SUMMARY:
Peak #1: Mean Diam.= 2.7 nm, S.Dev.= 0.4 nm (14.3%) Intens.= 1.1 %
Peak #2: Mean Diam.= 11.1 nm, S.Dev.= 2.3 nm (20.8%) Intens.= 25.1 %
Peak #3: Mean Diam.= 153.9 nm, S.Dev.= 32.4 nm (21.1%) Intens.= 73.8 %

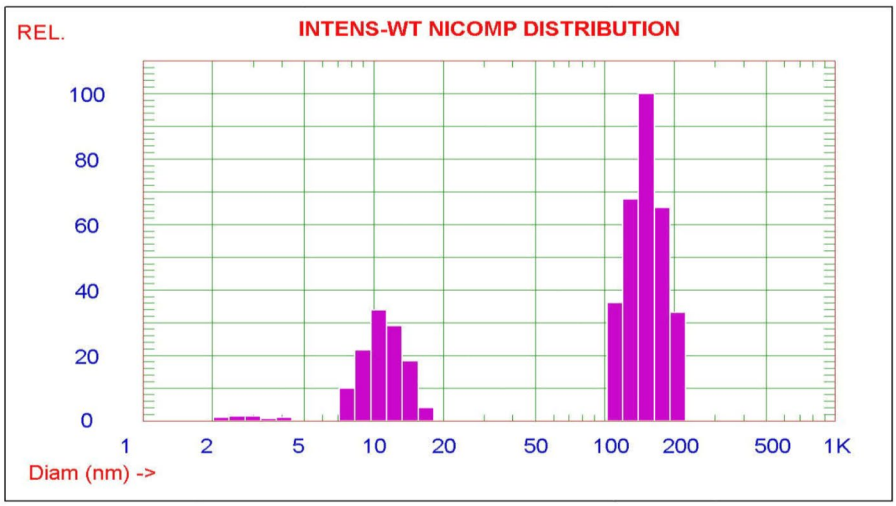

Run_Sample

Mean Diameter = 112.7 nm Fit Error = 6.496 Residual = 0.000

NICOMP SCALE PARAMETERS:
Min. Diam. = 1 nm Plot Size = 45
Smoothing = 3 Plot Range = 1000

GAUSSIAN SUMMARY:

Mean Diameter	*= 53.1 nm*	*Variance (P.I.)*	*= 0.731*
Stnd. Deviation	*= 45.4 nm (85.5%)*	*Chi Squared*	*= 1521.274*
Norm. Stnd. Dev.	*= 0.855*	*Baseline Adj.*	*= 0.000 %*
(Coeff. of Var'n)		*Z-Avg. Diff. Coeff.*	*= 8.75E-008 cm2/s*
Run Time	*= 0 Hr 2 Min 14 Sec*	*Wavelength*	*= 658.0 nm*
Count Rate	*= 100 KHz*	*Temperature*	*= 23 deg C*
Channel #1	*= 7.8 K*	*Viscosity*	*= 0.933 cp*
Channel Width	*= 6.4 uSec*	*Index of Ref*	*= 1.333*

Figure.4-12. Particle Size of the Optimized Liquid-SMEDDS

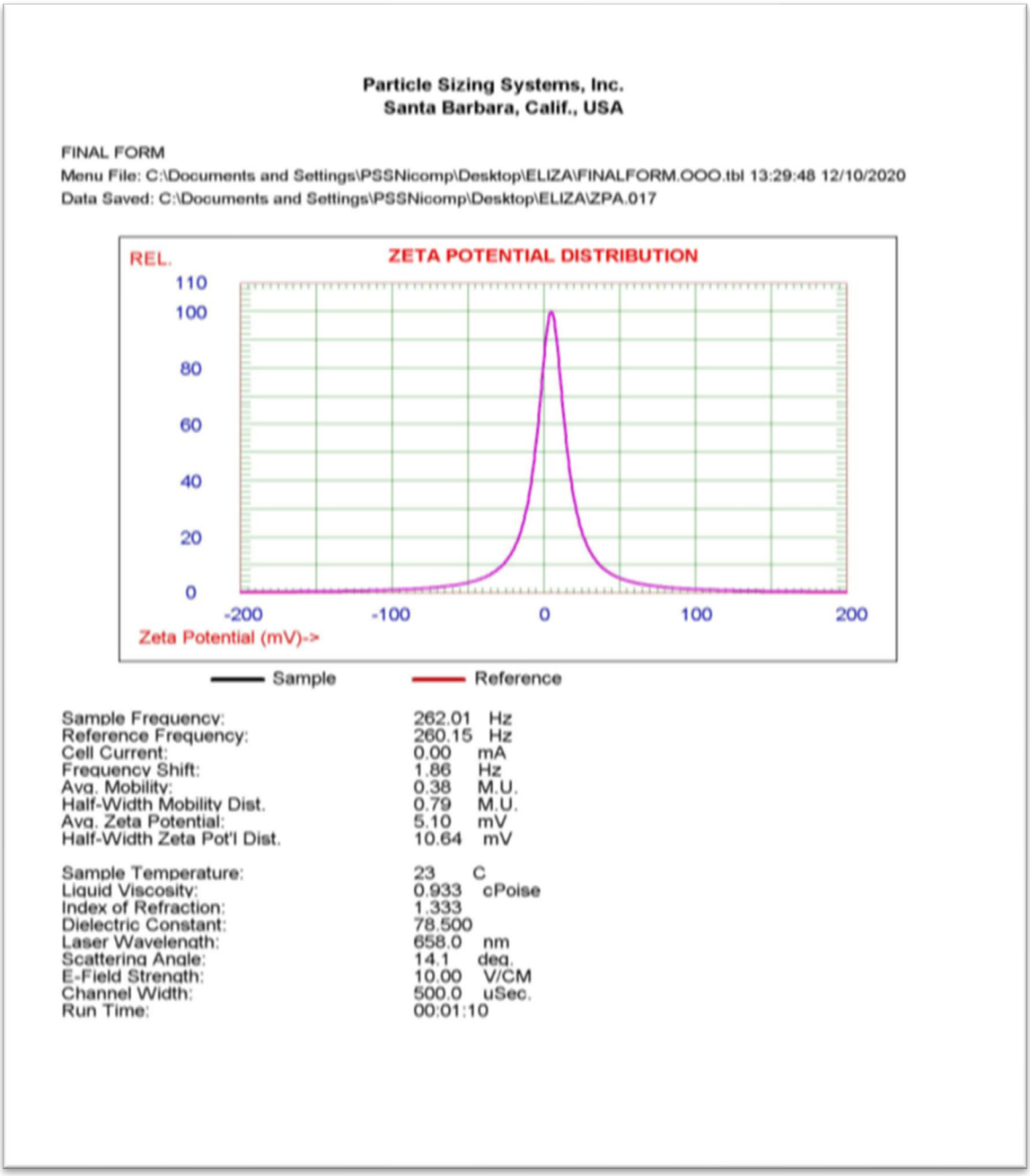

Figure.4-13. Zeta Potential of the Optimized Liquid-SMEDDS

4.6. Solid-SMEDDS Preparation and Characterization.

4.6.1. Solid-SMEDDS Preparation.

The adsorption capacity was determined to be 2.7 which falls between the reported adsorption capacity of Neuisiln US2 (2.7-3.4). The visual representation of the solid-SMEDDS is shown in figure.4.14. MMEO was well adsorbed unto Neusilin US2.

Figure.4-14 Solid-SMEDDS Picture.

4.6.2. Solid-SMEDDS Characterization.

There were no lipid-based instabilities like phase separation and oil precipitation observed with the reconstituted emulsion. The mean particle size of the microemulsion dispersion obtained from the solid-SMEDDS was 194.4 nm as seen in figure 4.15. This was still within acceptable limits for SMEDDS particle size (100nm to 250 nm). The increased particle size of this dispersion compared to microemulsions obtained from liquid-SMEDDS could be attributed to droplet growth in the emulsion.

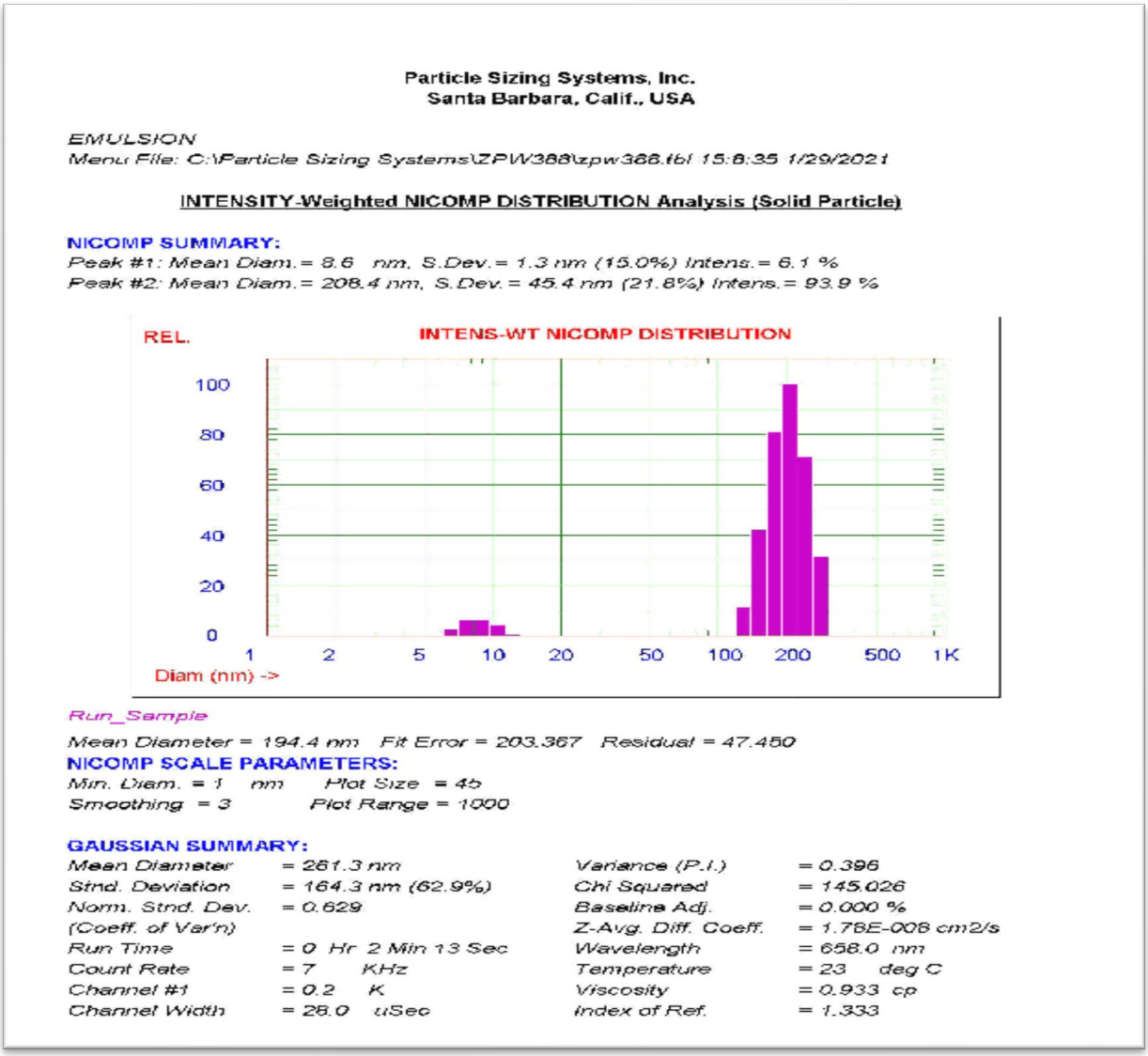

Figure.4-15. Mean Particle Size of Reconstituted Emulsion.

The intrinsic properties of powders such as size and shape, cohesiveness, a surface area greatly influence the density of powders (34). To correctly characterize the mechanical properties of a powder, true density is a fundamental property that has to be determined(35). To predict powder's flowability, the determination of the compressibility

index (CI) is the fastest way to achieve this. The compressibility index includes the Carr index and Hausner's ratio. For the solid-SMEDDS, true density was determined to be 1.12 ±0.01g/ml, bulk density was determined to be 0.24 ± 0.009 g/ml and tapped density was determined to be 0.30 ± 0.014 g/ml. Carr Index was determined to be 0.20 which indicates excellent flow and the Hausner ratio was determined to be 1.25 which indicates fair flow as interpreted from the information in table 4.8. The porosity of solid-SMEDDS was determined to be 78%. The flow of a powder during direct compression will greatly influence tablet weight and content uniformity(36).

Table 4. 8. Carr Index and Hausner Ratio (37).

Flow character of powders	**Hausner ratio (HR) Limits**	**Carr Index (CI) Limits**
Excellent	1.00–1.11	≤10
Good	1.12–1.18	11–15
Fair	1.19–1.25	16–20
Passable	1.26–1.34	21–25
Poor	>1.35	>26

4.6.1 Tablet Compression and Characterization.

4.6.1.1. Tablet Compression.

The angle of repose was determined for type1, type 2, and type 3 tablets using the carr classification of flowability of powder as shown in table 4.9. The angle of repose for type 1, type 2 and type 3 powder were determined to be 38.39 ±2.98°, 36.42 ±3.2°, and 34.53 ± 3.15° respectively. This indicates that the powder used for type 1 and type 2 tablet compression have fair flow while type 3 tablet is free-flowing.

Table 4. 9. Angle of Repose (38).

Description	Repose Angle
Very free-flowing	<30°
Free-flowing	30–38°
Fair to passable flow	38–45°
Cohesive	45–55°
Very cohesive (non-flowing)	>55°

The pictures of the different types of tablets compressed are shown in appendix A. From physically observing the tablets, it appeared as if type 3 tablets were well best directly compressed. The tablets were tried to be broken by hands and the greatest pressure was applied to the type 3 table. Table 4.10. shows the amount of each ingredient in each tablet. Type 3 contained only s-SMEDDS and cellulose.

Table 4. 10.Amount of the Ingredients in each S-SMEDDS Tablets.

	PHARMACEUTICAL USE	TYPE 1(mg/ tablet)	TYPE 2(mg/tablet)	TYPE 3(mg/tablet)	BLANK (mg/tablet)-type 2	Blank(mg/tablet)-type 3
S-SMEDDS	API	50	56	90	25	90
Micro crystalline cellulose	Binder	58	76	110	29	110
Spray Dried Lactose	Diluent	64	40		32	
Starch	Diluent	20	20		10	
Talc	Glidant	6	6		6	
Magnesium stearate	Lubricant	2	2		2	

4.6.1.2. Tablet Characterization.

All the tablet types as shown in figure 4.16. passed the weight variation test since none of the tablets was within the ±25 % difference limit and no tablet differed more than two times the limit as per USP requirement.

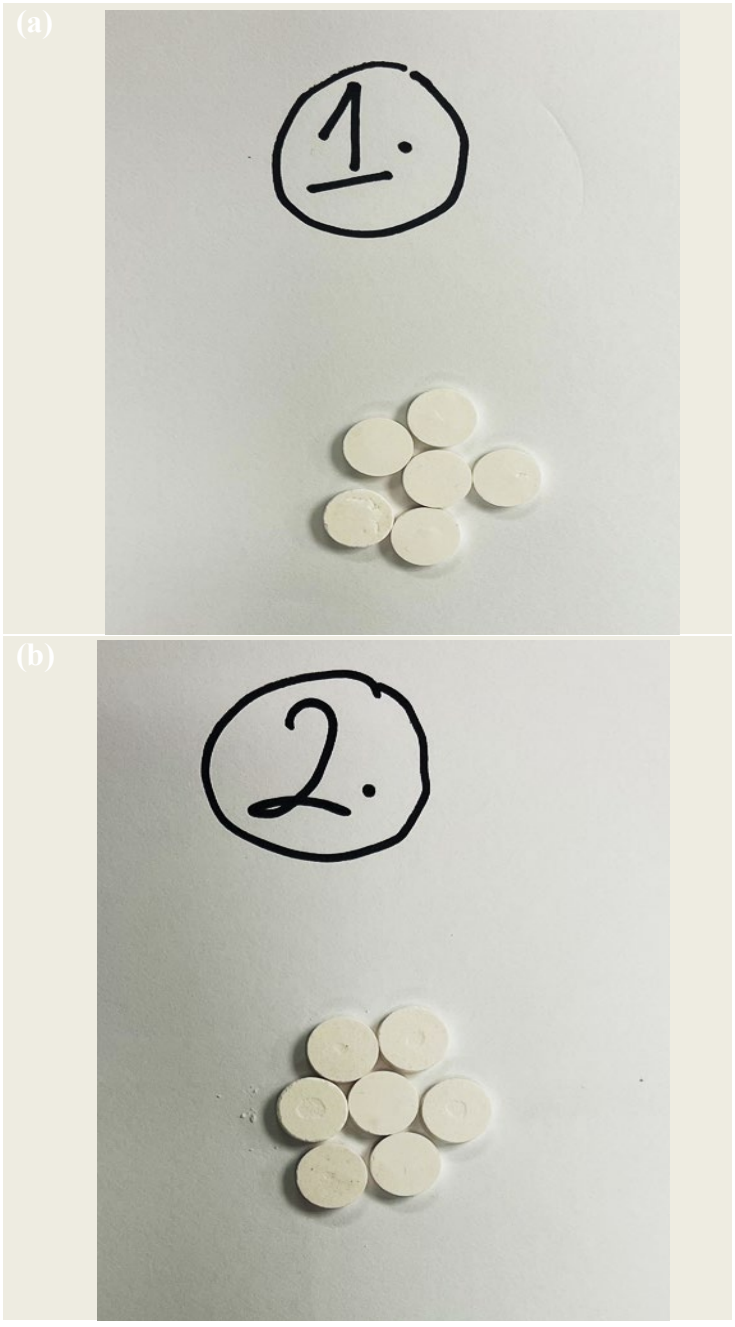

Figure 4-16. Pictures of (a) Type 1 Tablets (b) Type 2 Tablets (c) Type 3 Tablets.

The weight tablet characterization data can be seen in appendix A. The average weight for type 1 tablet was 0.188 g, type 2 tablet was 0.1878 g, and type 3 tablet was 0.170 g. Although it was seen that there was more variation with type 3 tablets with the highest percentage weight variation being 8.2 %. Weight variation can be used for content uniformity tests. Type 3 tablet had the smallest thickness which could be because of the different compressibility of the powders. The powders used did not compress and compact the same way. The smaller the tablet thickness, the higher the tablet breaking force. This is because a smaller distance between punches will allow for greater pressure for direct compression. The smaller the volume of powder (bulkiness), the punch can gets

closer to the die. This would explain why type 3 tablets are the hardest. The small distance between punches results in greater pressure applied for compression. Friability test is used to determine the level of stress a tablet can undergo without losing more than 1% of its original weight. According to USP pharmacopeia, tablets must not lose more than 1% of their original weight to pass the friability test. Type 3 tablets have the lowest % weight loss indicating it is the most compact. Type 3 has the largest breaking force and both types 1 and 2 have similar breaking force. Type 1 tablet disintegrated first, followed by type 2, and type 3 disintegrated last. Using one-way ANOVA, the P-value obtained was below 0.05 for tablet thickness, tablet breaking force, and disintegration tests. Therefore, there is a statistically significant difference between type 1, type, and type 3 tablets properties such as tablet thickness, tablet breaking force, and disintegration time. The P-value for the % friability was above 0.05. Thus, there is no significant difference in the % weight loss for type 1, type 2, and type 3 tablets as shown in table 4.11.

Table 4. 11. One-way ANOVA

ANOVA

		Sum of Squares	df	Mean Square	F	Sig.
thickness(mm)	Between Groups	.108	2	.054	121.675	<.001
	Within Groups	.003	6	.000		
	Total	.111	8			
% Friability	Between Groups	.205	2	.103	3.938	.081
	Within Groups	.156	6	.026		
	Total	.361	8			
Breaking Force(kg)	Between Groups	27.041	2	13.521	300.457	<.001
	Within Groups	.675	15	.045		
	Total	27.716	17			
Disin.test(min)	Between Groups	191.627	2	95.814	60.671	<.001
	Within Groups	23.689	15	1.579		
	Total	215.316	17			
Breaking Force(N)	Between Groups	790.111	2	395.056	23.500	<.001
	Within Groups	252.167	15	16.811		
	Total	1042.278	17			

Figure 4.17. shows the graph plot of type 1, type 2, and type 3 for average tablet thickness, friability, breaking force (manual and automatic), and disintegration time analysis.

The mean difference within groups was not done since the goal of the analysis was to compare type 1, type 2, and type 3 in general.

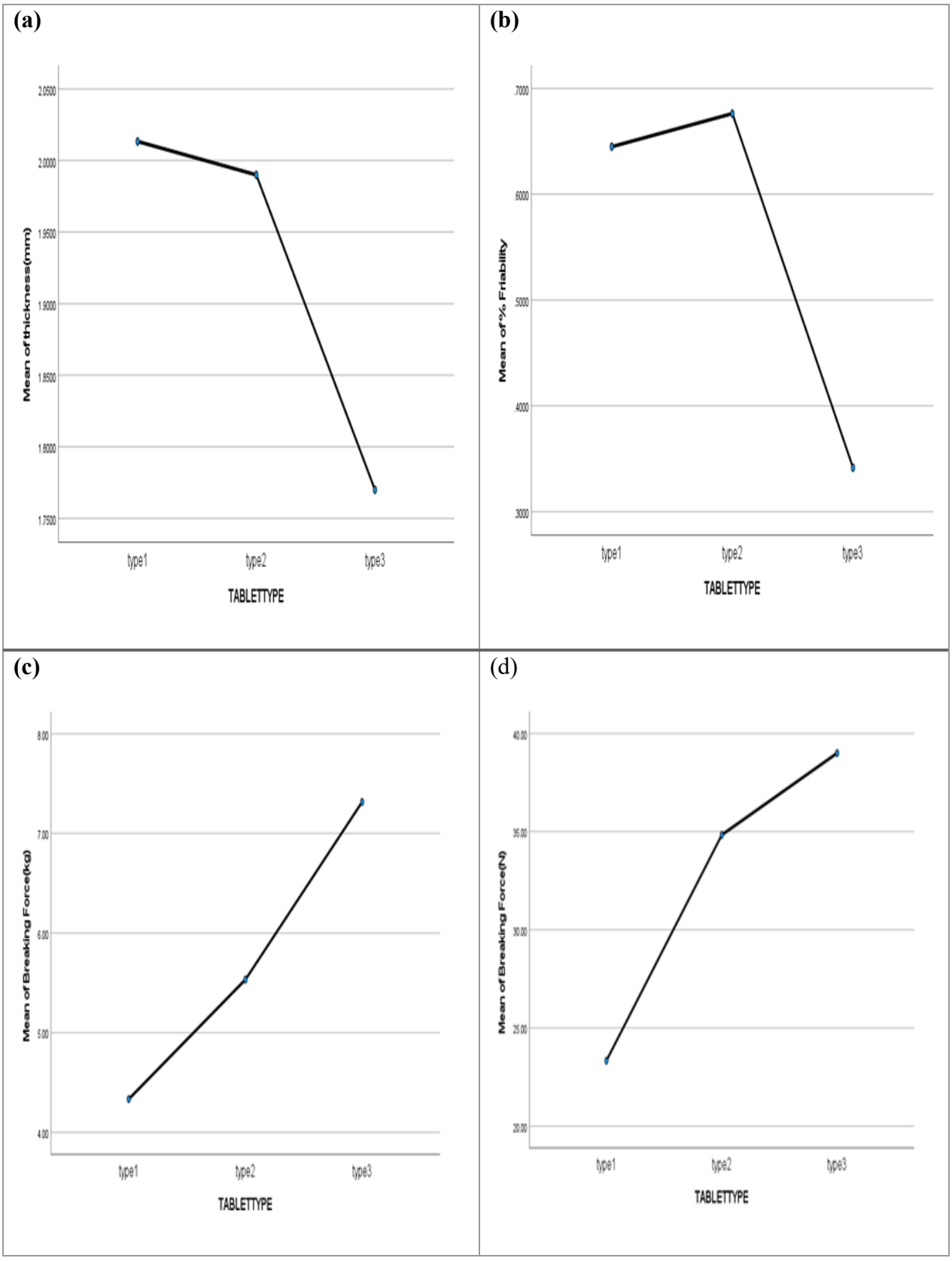
(a)
Mean of thickness(mm)
2.0500
2.0000
1.9500
1.9000
1.8500
1.8000
1.7500
type1
type2
type3
TABLETTYPE
(b)
Mean of % Friability
7.000
6.000
5.000
4.000
3.000
type1
type2
type3
TABLETTYPE
(c)
Mean of Breaking Force(kg)
8.00
7.00
6.00
5.00
4.00
type1
type2
type3
TABLETTYPE
(d)
Mean of Breaking Force(N)
40.00
35.00
30.00
25.00
20.00
type1
type2
type3
TABLETTYPE

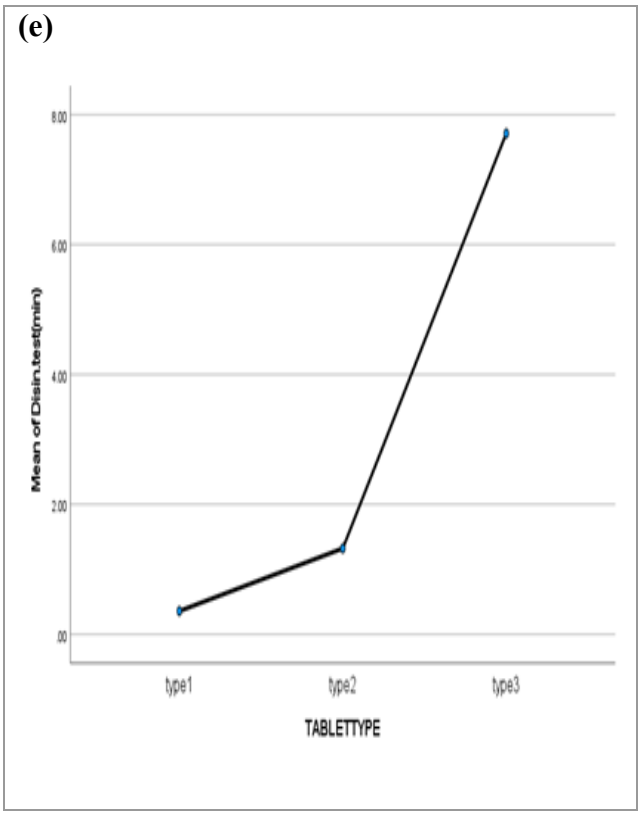

Figure 4-17. Mean Graphs for Type1, 2 and 3 Tablets: (a)Thickness(mm) (b) Friability (%) (c) Breaking Force-kg (d) Breaking Force-N (e) Disintegration Time (1)

4.7. Drug Content Analysis.

4.7.1. Calibration curve.

The highest absorbance was achieved at 243nm when screening from 200nm to 400nm. The absorbance derived for various concentrations can be seen in table.4.12. A calibration curve was generated as shown in figure 4.18. The equation of the graph was determined to be 0.0076x + 0.0543, with an r-squared value of 0.9953.

Table 4. 12 MMEO Absorbance

Concentration(milligram/ml)	Absorbance 1	Absorbance2	Absorbance 3	Average
31.25	0.287	0.289	0.289	0.288
15.625	0.180	0.181	0.180	0.180
7.1825	0.112	0.113	0.111	0.112
3.90625	0.077	0.077	0.077	0.077

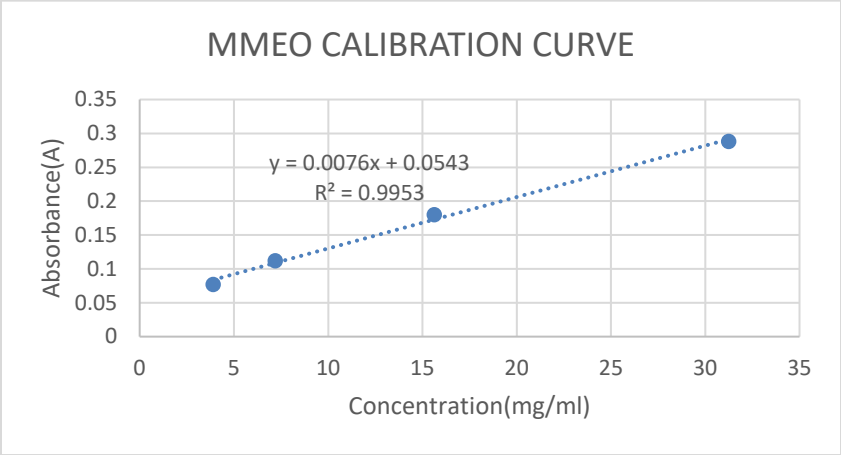

Figure 4-18. Calibration curve of MMEO

4.7.2. Drug Content.

Theoretically, the amount of MMEO was expected in each tablet was expected to be 0.513 mg for type 1, 0.575 mg for type 2, and 0.835 mg for type 3 as shown in the calculation below;

a. Type 1

The average weight of each tablet is 18.8 mg

The percentage of SMEDDS is 25 %

Amount of SMEDD= $[25/100] \times 18.8\, mg$

=4.7 mg.

Amount of MMEO = $\left[\frac{10.92}{100}\right] \times 4.7mg$

=**0.513 mg**

b. Type 2

The average weight of each tablet is 18.7 mg

The percentage of SMEDDS is 28 %

Amount of SMEDD= $[28/100] \times 18.8\ mg$

=5.264 mg.

Amount of MMEO = $\left[\frac{10.92}{100}\right] \times 5.264mg$

=**0.575 mg**

c. Type 3

The average weight of each tablet is 17.0 mg

The percentage of SMEDDS is 45 %

Amount of SMEDD= $[45/100] \times 17.0\ mg$

=7.65mg.

Amount of MMEO = $\left[\frac{10.92}{100}\right] \times 7.65\ mg$

=0.835 mg

The absorbance and MMEO amount can be over the 3 weeks can be seen in appendix c. For the first week, type 1 had 0.355 ± 0.00 mg, type 2 had 0.352 ± 0.000 mg, type 3 had 0.750 ± 0.000 mg of MMEO. This was comparable with the second-week amount of MMEO estimate where type 1 had 0.355 ± 0.000 mg, type 2 had 0.131 ± 0.000 mg, and type 3 had 0.798 ± 0.000 mg of MMEO. Type 2 was a bit different which could be because

of molecular interaction among the tablet ingredients. This would also explain why there was a negative value of MMEO for type 1 (-3.7625±0.000) and type 2 (- 4.33 ± 0.000) tablets in the third week. Only type 3 tablets had the highest and most uniform MMMEO content over the three weeks. The drug content data can be seen in Appendix B.

4.8. Fourier Transfer Infrared Spectroscopy (FTIR).

Interpretations of the peaks were done using the functional group region (4000 cm-1 to 1450 cm-1) of the IR spectra. Characteristics peaks of 3391.15, 2958.64, 1457.15, 1367.12 /cm were seen for MMEO. A peak at 3391.15 indicates –OH (alcohol) stretching or a strong -NH (primary amine) stretching. The medium peak at 2985.64 indicates -OH (carboxylic) stretching or a strong -CH (alkane) stretching. A strong peak at 1457.15 indicates - CH bending. A medium peak at 1367.71 in the fingerprint region indicates -S=O (sulfonamide) Stretching. Strong- O-H (phenol or carboxylic) bending. For MMEO emulsion, characteristic peaks were seen at 3443.66, 2867.11, 1956.17, 1735.65, 1651.18, 1456.04. The Peak at 3443.66 indicates -OH (alcohol) stretching or a strong -N-H (primary amine) stretching. The medium peak at 2867.11 indicates -OH (carboxylic) stretching or a strong - N-H (primary amine) stretching. Strong peak at 1956.17 indicates-N=C=S (isothiocyanate) stretching or strong -C=C=C (allene) stretching. A strong peak at 1735.65 indicates -C=O (ester) stretching or a strong - C-H (aromatic compounds) bending. Strong. The peak at 1651.18 indicates C=O (δ-lactam) stretching or - C=C (conjugated alkene) stretching. The multitude of IR spectra peaks of MMEO could be due to several compounds present in MMEO. Some of the peaks present in MMEO IR spectra are absent in the emulsion spectra which indicates a molecular interaction or encapsulation within emulsion

droplets. Analysis of the IR spectra was done using Chemistry Libre text and spectroscopic tools software. The IR spectra of MMEO and emulsion can be seen in Appendix C.

4.9. Differential Scanning Calorimetry (DSC).

The analyzed thermograms for DSC of MMEO, liquid-SMEDDS, neusilin US2, and solid-SMEDDS can be seen in figure.4.19. MMEO showed an endothermic 39.25 °C. MMEO started undergoing phase transition at 82.22°C with a broad peak at 95.58°C. The broad peak of MMEO could be due to its complex composition and the oil evaporated after the first run. The first cycle of the liquid-SMEDDS showed that it first started melting at -3.08°C with a peak at -1.97°C, followed by crystallization at 0.59°C with a peak at 0.39. A glass transition phase for liquid-SMEDDS was seen at 9.6°C to 11.01°C with a peak point at 20.15°C and recrystallized at a peak temperature of 99.73°C. The cooling cycle showed crystallization occurring at a peak temperature of -31.96°C and a peak melting temperature of -7.72°C. The peaks present in the MMEO thermogram were absent in the liquid-SMEDDS thermogram indicating molecular interaction among the ingredients. Neusilin US2 indicated a phase transition at 162.98°C with a broad peak at 192.26°C. The solid-SMEDDS glass transition phase started at 139.49°C with a sharp melting point at 288.74°C. Solid-SMEDDS thermogram showed no representation of MMEO indicating the molecularity dispersion of MMEO in the optimized solid-SMEDDS.

(a)

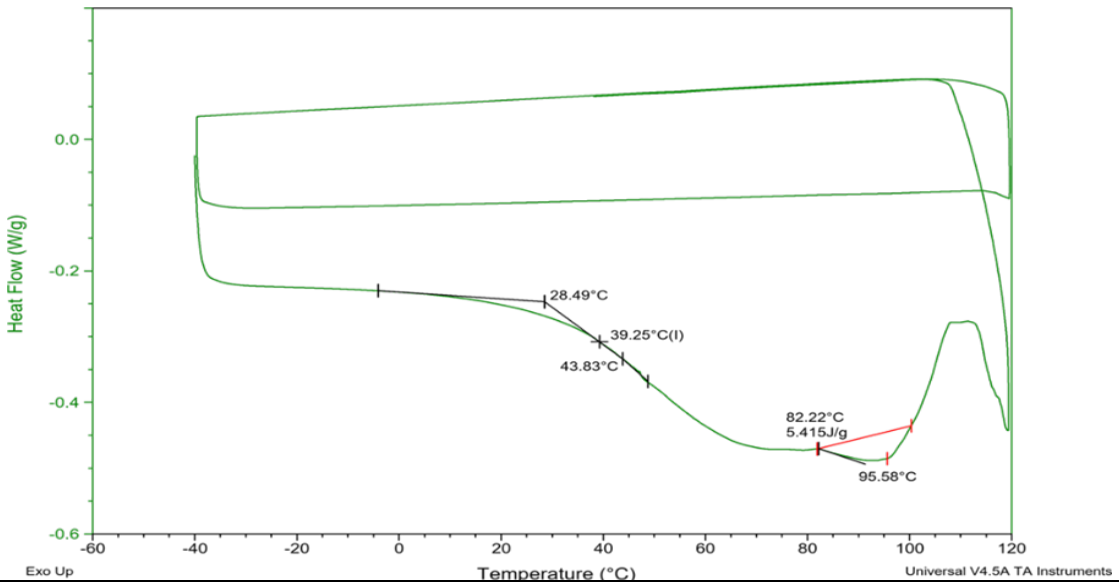
Heat Flow (W/g)
0.0
-0.2
-0.4
-0.6
28.49°C
39.25°C(I)
43.83°C
82.22°C
5.415J/g
95.58°C
-60
-40
-20
0
20
40
60
80
100
120
Exo Up
Temperature (°C)
Universal V4.5A TA Instruments

(b)

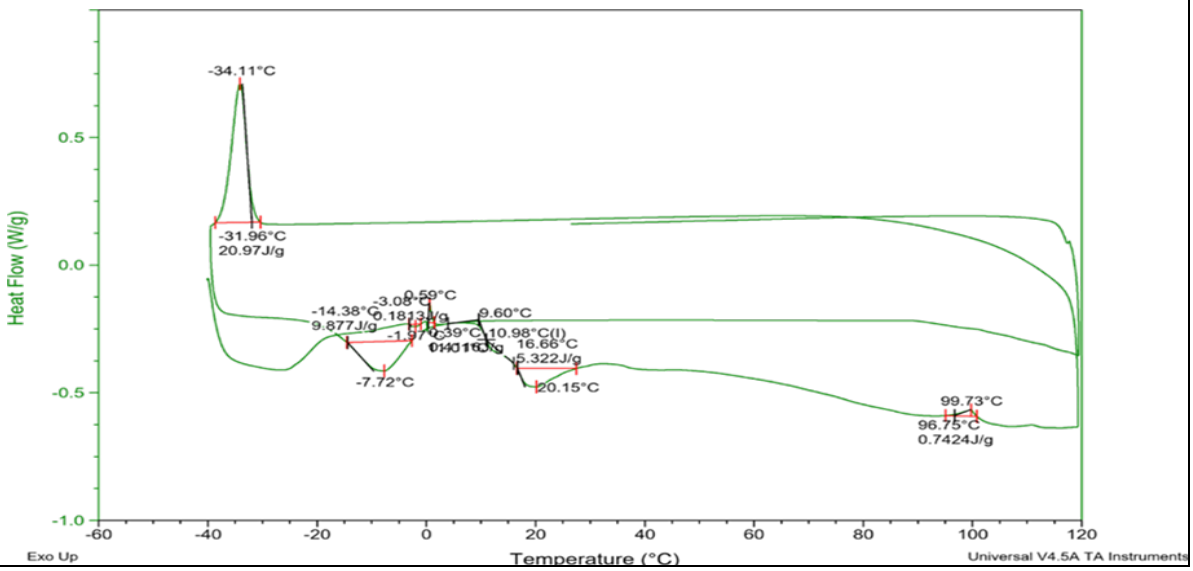
Heat Flow (W/g)
0.5
0.0
-0.5
-1.0
-34.11°C
-31.96°C
20.97J/g
-14.38°C
9.877J/g
-7.72°C
9.60°C
10.98°C(I)
16.66°C
5.322J/g
20.15°C
99.73°C
96.75°C
0.7424J/g
-60
-40
-20
0
20
40
60
80
100
120
Exo Up
Temperature (°C)
Universal V4.5A TA Instruments

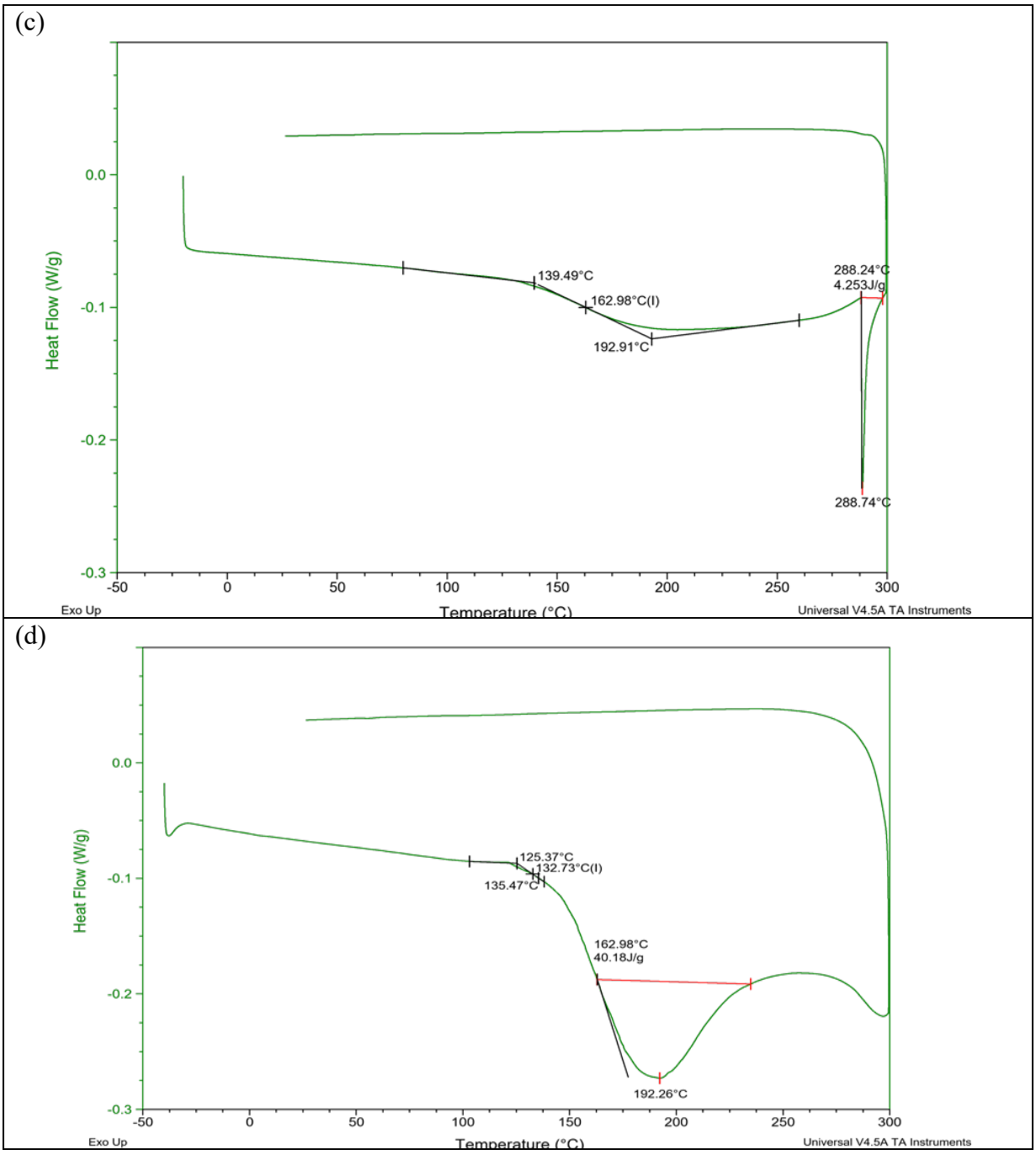

Figure 4-19. DSC Analysis of (a) MMEO (b) liquid-SMEDDS (c) Solid-SMEDDS (d) Neusilin US2.

4.10. Scanning Electron Microscopy (SEM).

The MMEO emulsion has two shapes (micelles and rods) as seen in figure.4.20. Microemulsion droplets can have either spherical or non-spherical (cylinder-like) shapes because of the reduced interfacial area, unlike nano-emulsion droplets that are generally spherically (39). The various shapes can also explain the wide range of droplet sizes observed with dynamic light scattering analysis. The rod-like shape could have been due to the drying process while experimenting. Morphology analysis of neusilin US2 showed perfectly spherical shapes and different sizes as seen in figure 4.20. Neusilin US2 is amorphous in nature. SEM analysis of solid-SMEDDS showed complete adsorption of the liquid-SMEDDS as shown in figure 4.20. Solid-SMEDDS is amorphous with spherical powder composition. SEM morphology of type 1, type2, and type 3 tablets can be seen in figure 4.20. Higher magnification of SEM of type 3 tablet can be seen in figure 4.20 also. The pictures show that the type 3 tablet was the most compact form of all the tablets. A closer view of the type 3 tablet shows the powder particles are perfectly uniform in shape unlike type 1 and 2 tablets that have some non-spherical powder particles.

(a)

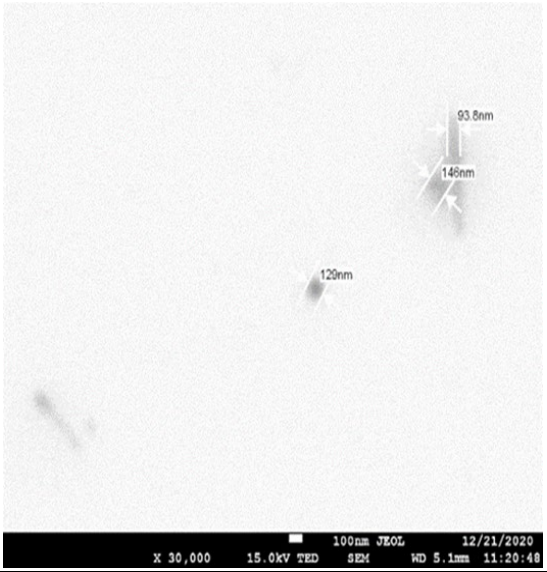
93.8nm
146nm
129nm
100nm JEOL 12/21/2020
X 30,000 15.0kV TED SEM WD 5.1mm 11:20:48

(b)

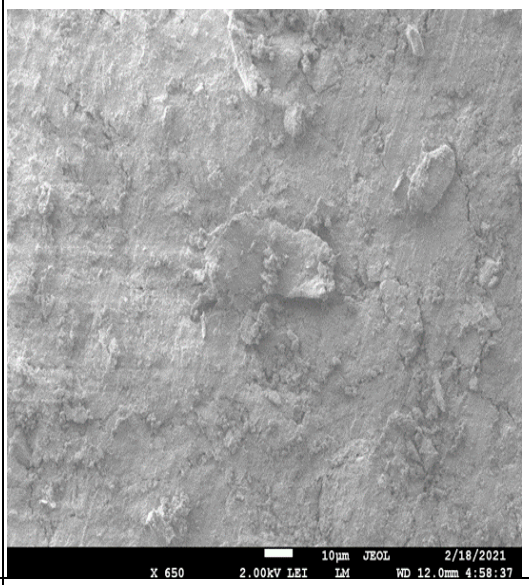
10µm JEOL 2/18/2021
X 650 2.00kV LEI LM WD 12.0mm 4:58:37

(c)

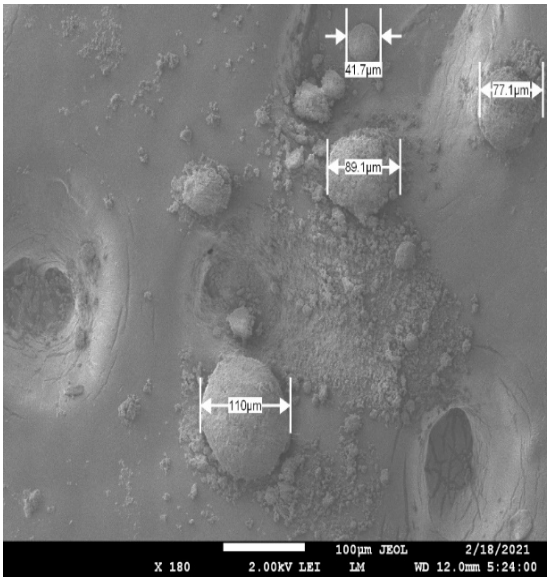
41.7µm
77.1µm
89.1µm
110µm
100µm JEOL 2/18/2021
X 180 2.00kV LEI LM WD 12.0mm 5:24:00

(d)

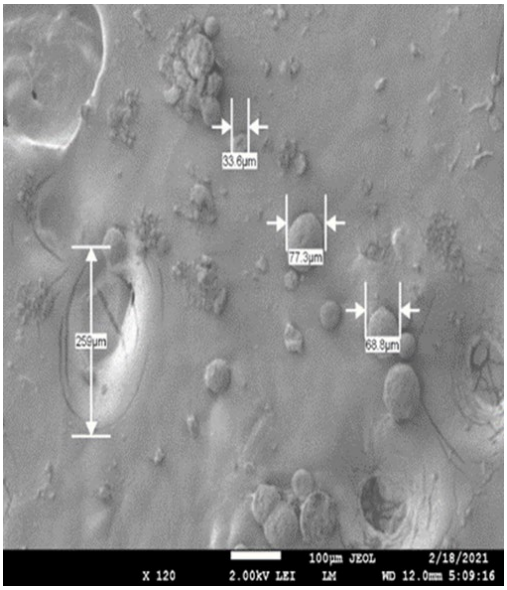
33.6µm
77.3µm
259µm
68.8µm
100µm JEOL 2/18/2021
X 120 2.00kV LEI LM WD 12.0mm 5:09:16

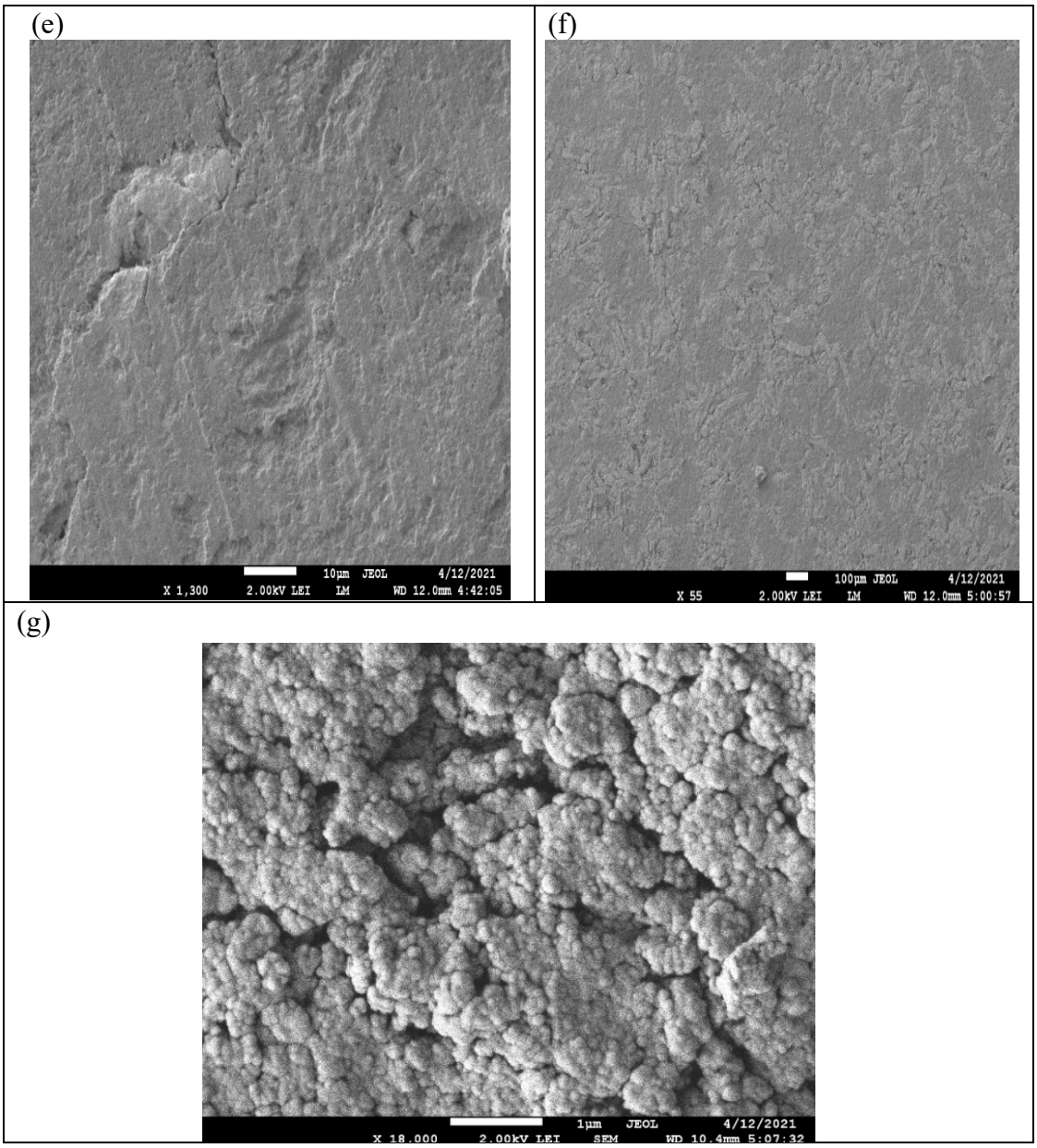

Figure 4-20: SEM images of (a) MMEO emulsion, (b) Neusilin (c) solid-SMEDDS (d) Type 1 tablet (e) Type 2 tablet (f) Type 3 tablet (g) Type 3 tablet at higher resolution.

Chapter 5

Conclusion

MMEO (10.92%) / Tween 80 (48%) / Transcutol HP (41.8%) was predicted to be the best formulation with desirable characteristics such as a mean particle size of 112.7 nm, the zeta potential of +5.10 mv, and a transparent emulsion. Easier product transport, better accurate dosing, stability of essential oils, and better patient compliance are some of the reasons why solidifying liquid-SMEDDS is becoming a popular opinion (40). Type 1, 2, and 3 tablets were directly compressed using various ingredients and ratios. Type 3 tablets showed the best characteristics desired and had the highest MMEO content. Using one-way ANOVA, the P-value obtained was below 0.05 for tablet thickness, tablet breaking force, and disintegration tests. Therefore, there is a statistically significant difference between type 1, type, and type 3 tablets properties such as tablet thickness, tablet breaking force, and disintegration time. The P-value for the % friability was above 0.05. Thus there is no significant difference in the % weight loss for type 1, type 2, and type 3 tablets. A tablet-loaded SMEDDS formulation is a promising approach to deliver essential oils (poorly soluble drugs). From this study, it was seen that the use of other excipients such as cellulose, starch, lactose, talc, magnesium stearate did not improve the physicochemical properties of type 1 and type 2 tablets. It can be inferred that type 3 tablet design should be adopted for further studies. Solid-SMEDDS can also be filled into capsule shells and

comparative studies can be done with type 3 tablets. In-vivo bioavailability studies can be done to better understand the type-3 tablets. In-vivo bioavailability studies can also be done to better understand the type-3 tablets. Animal studies to test for the pharmacology properties like; Alzheimer's disease, anticancer, antioxidant, and antimicrobial properties of the formulation may be done in the future.

References

1. Sutton AT, Kriewall CS, Leu MC, Newkirk JW. Powder characterisation techniques and effects of powder characteristics on part properties in powder-bed fusion processes. Virtual and physical prototyping. 2017;12(1):3-29.

2. Adewole E, Ajiboye B, Idris O, Ojo O, Onikan A, Ogunmodede O, et al. Phytochemical, Antimicrobial and Gc-Ms of African Nutmeg (Monodora Myristica). Phytochemical, Antimicrobial and Gc-Ms of African Nutmeg (Monodora Myristica). 2013;2(5):1-8.

3. Oyinloye BE, Adenowo AF, Osunsanmi FO, Ogunyinka BI, Nwozo SO, Kappo AP. Aqueous extract of Monodora myristica ameliorates cadmium-induced hepatotoxicity in male rats. SpringerPlus. 2016;5(1):1-7.

4. Obonga WO, Omeje EO, Nnadi CO, Ocheme WG. Phytochemical Evaluation of Extracts and GC-MS analysis of oil from Monodora myristica Seed. Dhaka University Journal of Pharmaceutical Sciences. 2019;18(1):69-73.

5. Owokotomo IA, Ekundayo O. Comparative study of the essential oils of Monodora myristica from Nigeria. European Chemical Bulletin. 2012;1(7):263-5.

6. Erukainure O, Ajiboye J, Abbah U, Asieba G, Mamuru S, Zaruwa M, et al. Monodora myristica (African nutmeg) modulates redox homeostasis and alters functional

chemistry in sickled erythrocytes. Human & experimental toxicology. 2018;37(5):458-67.

7. Ajayi I, Adebowale K, Dawodu F, Oderinde R. A study of the oil content of Nigerian grown Monodora myristica seeds for its nutritional and industrial applications. Biological Sciences-PJSIR. 2004;47(1):60-5.

8. Feyisayo AK, Oluokun OO. Evaluation of antioxidant potentials of Monodora myristica (Gaertn) dunel seeds. African Journal of Food Science. 2013;7(9):317-24.

9. Ekeanyanwu RC, Nkwocha CC, Ekeanyanwu CL. Behavioural and biochemical indications of the antidepressant activities of essential oils from Monodora myristica (Gaertn) seed and Xylopia aethiopica (Dunal) fruit in rats. IBRO Neuroscience Reports. 2021;10:66-74.

10. Owokotomo I, Ekundayo O, Abayomi T, Chukwuka A. In-vitro anti-cholinesterase activity of essential oil from four tropical medicinal plants. Toxicology reports. 2015;2:850-7.

11. Akinwunmi K, Oyedapo O. In vitro anti-inflammatory evaluation of African nutmeg (Monodora myristica) seeds. European Journal of Medicinal Plants. 2015:167-74.

12. Al-Tannak N, Khadra I, Igoli N, Igoli J. LC-MS analysis of oils of Monodora myristica and Monodora tenuifolia and isolation of a novel cyclopropane fatty acid. Natural product research. 2020;34(9):1227-32.

13. Market CG. 2021 [Available from: https://carrygomarket.com/products/ground-ehuru-african-nutmeg?_pos=2&_sid=183fe10e4&_ss=r&variant=13951218712694.

14. Dokania S, Joshi AK. Self-microemulsifying drug delivery system (SMEDDS)–challenges and road ahead. Drug delivery. 2015;22(6):675-90.

15. Balakumar K, Raghavan CV, Abdu S. Self nanoemulsifying drug delivery system (SNEDDS) of rosuvastatin calcium: design, formulation, bioavailability and pharmacokinetic evaluation. Colloids and Surfaces B: Biointerfaces. 2013;112:337-43.

16. Almoazen H. Felton L. Remington: Essentials of Pharmaceutics. Pharmaceutical Press; 2013, 772pp, $69.00 (softcover), ISBN 9780857111050. American Journal of Pharmaceutical Education; 2013.

17. Staden Dv, Du Plessis J, Viljoen J. Development of topical/transdermal self-emulsifying drug delivery systems, not as simple as expected. Scientia Pharmaceutica. 2020;88(2):17.

18. Pouton CW. Formulation of self-emulsifying drug delivery systems. Advanced drug delivery reviews. 1997;25(1):47-58.

19. AboulFotouh K, Allam AA, El-Badry M, El-Sayed AM. Development and in vitro/in vivo performance of self-nanoemulsifying drug delivery systems loaded with candesartan cilexetil. European Journal of Pharmaceutical Sciences. 2017;109:503-13.

20. Radha G, Sastri KT, Burada S, Rajkumar J. A systematic review on self-micro emulsifying drug delivery systems: A potential strategy for drugs with poor oral bioavailability. Int J App Pharm. 2019;11:23-33.

21. Cilliers L. Development and evaluation of a self-emulsifying drug delivery system for artemether and lumefantrine: North-West University (South-Africa); 2019.

22. McClements DJ. Nanoemulsions versus microemulsions: terminology, differences, and similarities. Soft matter. 2012;8(6):1719-29.

23. Chatterjee B, Hamed Almurisi S, Ahmed Mahdi Dukhan A, Mandal UK, Sengupta P. Controversies with self-emulsifying drug delivery system from pharmacokinetic point of view. Drug delivery. 2016;23(9):3639-52.

24. Kollipara S, Gandhi RK. Pharmacokinetic aspects and in vitro–in vivo correlation potential for lipid-based formulations. Acta Pharmaceutica Sinica B. 2014;4(5):333-49.

25. Wu L, Qiao Y, Wang L, Guo J, Wang G, He W, et al. A self-microemulsifying drug delivery system (SMEDDS) for a novel medicative compound against depression: a preparation and bioavailability study in rats. AAPS PharmSciTech. 2015;16(5):1051-8.

26. Sailor GU. Self-Nanoemulsifying Drug Delivery Systems (SNEDDS): An Innovative Approach to Improve Oral Bioavailability. In: Shah N, editor. Nanocarriers: Drug Delivery System: An Evidence Based Approach. Singapore: Springer Singapore; 2021. p. 255-80.

27. Guenther E. The essential oils. Vol. 5. The essential oils Vol 5. 1952.

28. Ekere N, Odoemelam C, Ihedioha J, Okoye C. Profile of seed oils from Monodora myristica and Monodora tenuifoila plants. Journal of Chemical Society of Nigeria. 2015;40(2).

29. Pouton CW. Lipid formulations for oral administration of drugs: non-emulsifying, self-emulsifying and 'self-microemulsifying'drug delivery systems. European journal of pharmaceutical sciences. 2000;11:S93-S8.

30. Rahardiyan D, Poluakan M, Moko EM. Physico-chemical Properties of Nutmeg (Myristica fragrans houtt) of North Sulawesi Nutmeg. Fullerene Journal of Chemistry. 2020;5(1):23-31.

31. Akise Ogheneughwe Godwin FEAaAEO. Phytochemical Properties of Essential Oils of Ginger (Zingiber officinale), African Nutmeg (Monodora myristica) and Ashanti Black Pepper (Piper guineense). Advance Journal of Food Science and Technology. 2019;4:58-64.

32. Hashiba A, Toyooka M, Sato Y, Maeki M, Tokeshi M, Harashima H. The use of design of experiments with multiple responses to determine optimal formulations for in vivo hepatic mRNA delivery. Journal of Controlled Release. 2020;327:467-76.

33. Čerpnjak K, Zvonar A, Gašperlin M, Vrečer F. Lipid-based systems as promising approach for enhancing the bioavailability of poorly water-soluble drugs. Acta pharmaceutica. 2013;63(4):427-45.

34. e Silva JS, Splendor D, Gonçalves I, Costa P, Lobo JS. Note on the measurement of bulk density and tapped density of powders according to the European Pharmacopeia. Aaps Pharmscitech. 2013;14(3):1098-100.

35. Sun CC. A material-sparing method for simultaneous determination of true density and powder compaction properties—Aspartame as an example. International journal of pharmaceutics. 2006;326(1-2):94-9.

36. Prescott JK, Barnum RA. On powder flowability. Pharmaceutical technology. 2000;24(10):60-85.

37. Kaleem MA, Alam MZ, Khan M, Jaffery SHI, Rashid B. An experimental investigation on accuracy of Hausner Ratio and Carr Index of powders in additive manufacturing processes. Metal Powder Report. 2020.

38. Al-Hashemi HMB, Al-Amoudi OSB. A review on the angle of repose of granular materials. Powder technology. 2018;330:397-417.

39. Pavoni L, Perinelli DR, Bonacucina G, Cespi M, Palmieri GF. An overview of micro-and nanoemulsions as vehicles for essential oils: Formulation, preparation and stability. Nanomaterials. 2020;10(1):135.

40. Mandić J, Pobirk AZ, Vrečer F, Gašperlin M. Overview of solidification techniques for self-emulsifying drug delivery systems from industrial perspective. International journal of pharmaceutics. 2017;533(2):335-45.

41. Sinka I, Motazedian F, Cocks A, Pitt K. The effect of processing parameters on pharmaceutical tablet properties. Powder Technology. 2009;189(2):276-84.

Appendix A

Tablet Characterization

Table A. 1. Weight Variation of Type 1, 2, and 3 Tablets.

TABLET NO	TYPE 1 Average Weight- 0.188g		TYPE 2 Avg Weight-0.187g		TYPE 3 Avg Weight- 0.170g	
	Weight (gram)	% difference	Weight (gram)	% difference	Weight (gram)	% difference
1	0.190	1.064	0.188	0.532	0.169	0.588
2	0.190	1.064	0.185	1.070	0.160	5.882
3	0.188	0.000	0.184	1.604	0.180	5.882
4	0.189	0.532	0.189	1.070	0.170	0.000
5	0.191	1.596	0.188	0.532	0.163	4.118
6	0.191	1.596	0.186	0.100	0.172	1.176
7	0.189	0.532	0.184	1.064	0.184	8.235
8	0.186	1.064	0.190	1.604	0.161	5.294
9	0.189	0.532	0.187	0.000	0.169	0.558
10	0.184	2.128	0.186	0.100	0.163	4.118
11	0.189	0.532	0.189	1.100	0.172	1.176
12	0.183	2.659	0.186	0.100	0.183	7.657
13	0.183	2.659	0.185	1.070	0.169	0.588

14	0.187	0.532	0.185	1.070	0.178	4.706
15	0.192	2.128	0.191	2.140	0.165	2.941
16	0.187	0.532	0.192	2.674	0.165	2.941
17	0.189	0.532	0.184	1.604	0.164	2.732
18	0.184	2.127	0.184	1.604	0.183	7.647
19	0.187	0.532	0.187	0.000	0.165	2.186
20	0.190	1.064	0.190	1.604	0.165	2.941

Table A. 2. Tablet Thickness of Type 1, 2, and 3.

TYPE 1 (mm)	TYPE 2 (mm)	TYPE 3 (mm)
2.00	1.99	1.80
2.01	2.01	1.75
2.03	1.97	1.76

Table A. 3. Tablet Percentage Friability of Type 1, 2, and 3.

	Initial Weight (g)	Final Weight (g)	% Weight loss
Type 1	6.650	6.608	0.632
	6.751	6.715	0.533
	6.621	6.571	0.770
Type 2	6.801	6.738	0.926
	6.735	6.699	0.534
	6.679	6.641	0.569
Type 3	6.859	6.831	0.409
	6.839	6.810	0.424
	6.778	6.765	0.1917

Table A. 4. Tablet Breaking Force Test for Type 1, 2, and 3.

TYPE	Manual Instrument(41)		Digital electronic breaking force tester (newtons)
TYPE 1	1	4.5	23
	2	4	22
	3	4.5	28
	4	4.5	23
	5	4	22
	6	4.5	23
TYPE 2	1	5.6	39
	2	5.5	37
	3	5.5	25
	4	5.6	36
	5	5.4	33
	6	5.6	39
TYPE 3	1	7.5	41
	2	7.5	40
	3	7.0	41
	4	7.4	34
	5	7.0	34
	6	7.5	44

Table A. 5. Type1,2 and 3 Disintegration Test

S/N	TYPE 1		TYPE 2		TYPE 3	
	Weight (mg)	Time (sec)	Weight(mg)	Time (sec)	Weight (mg)	Time (sec)
1	181	0.28	185	1.41	164	7.8
2	178	0.56	182	1.25	165	6.8

3	183	0.28	191	1.24	170	10.37
4	181	0.45	187	1.25	161	9.89
5	186	0.29	184	1.29	168	6.9
6	186	0.29	183	1.50	183	4.51

Table A. 6. Type 1, 2, and 3 tablets mean and standard deviation.

Descriptives

						95% Confidence Interval for Mean			
		N	Mean	Std. Deviation	Std. Error	Lower Bound	Upper Bound	Minimum	Maximum
thickness(mm)	type1	3	2.013333	.0152753	.0088192	1.975388	2.051279	2.0000	2.0300
	type2	3	1.990000	.0200000	.0115470	1.940317	2.039683	1.9700	2.0100
	type3	3	1.770000	.0264575	.0152753	1.704276	1.835724	1.7500	1.8000
	Total	9	1.924444	.1176978	.0392326	1.833974	2.014915	1.7500	2.0300
% Friability	type1	3	.645000	.1190336	.0687241	.349304	.940696	.5330	.7700
	type2	3	.676333	.2169247	.1252415	.137462	1.215204	.5340	.9260
	type3	3	.341567	.1300049	.0750583	.018617	.664517	.1917	.4240
	Total	9	.554300	.2125369	.0708456	.390930	.717670	.1917	.9260
Breaking Force(kg)	type1	6	4.3333	.25820	.10541	4.0624	4.6043	4.00	4.50
	type2	6	5.5333	.08165	.03333	5.4476	5.6190	5.40	5.60
	type3	6	7.3167	.24833	.10138	7.0561	7.5773	7.00	7.50
	Total	18	5.7278	1.27686	.30096	5.0928	6.3627	4.00	7.50
Disin.test(min)	type1	6	.3583	.11890	.04854	.2336	.4831	.28	.56
	type2	6	1.3233	.10727	.04379	1.2108	1.4359	1.24	1.50
	type3	6	7.7117	2.17073	.88620	5.4336	9.9897	4.51	10.37
	Total	18	3.1311	3.55888	.83884	1.3613	4.9009	.28	10.37
Breaking Force(N)	type1	6	23.3333	2.33809	.95452	20.8797	25.7870	22.00	28.00
	type2	6	34.8333	5.30723	2.16667	29.2637	40.4029	25.00	39.00
	type3	6	39.0000	4.09878	1.67332	34.6986	43.3014	34.00	44.00
	Total	18	32.3889	7.83010	1.84557	28.4951	36.2827	22.00	44.00

Appendix B

Drug Content

Table B. 1: Amount of MMEO in Type 1, 2, and 3 Tablets for Week 1.

	Type 1	Type 2	Type 3
Weight (g)	186	184	163
	184	185	161
	185	182	169
Average	185	183.7	164.3
Absorbance (A)	0.058	0.057	0.060
	0.057	0.055	0.063
	0.056	0.055	0.057
Average	0.057±0.000	0.055±0.000	0.060±0.000
Amount (mg)	0.355±0.000	0.352±0.000	0.750±0.003

Table B. 2: Absorbance of Type 1, 2, and 3 Tablets for Week 2.

	Type 1	Type 2	Type 3
Weight (g)	189	186	165
	191	191	164
	185	186	165
Average	188.3	187.6	164.7
Absorbance (A)	0.056	0.055	0.060
	0.056	0.054	0.060
	0.057	0.056	0.061
	0.057±0.000	0.055±0.000	0.063±0.001
Amount(mg)	0.355±0.000	0.131±0.000	0.798±0.000

Table B. 3: Absorbance of Type 1, 2, and 3 Tablets for Week 3.

	Type 1	Type 2	Type 3
Weight (mg)	195	184	164
	184	185	156

	187	184	162
Average	188.6	184.3	160.7
Absorbance (A)	0.027	0.020	0.060
	0.025	0.021	0.060
	0.025	0.023	0.060
	0.026±0.000	0.021±0.000	0.060±0.000
Amount(mg)	-3.7675±0.000	-4.33 ±0.000	0.750±0.000

Appendix C

FTIR

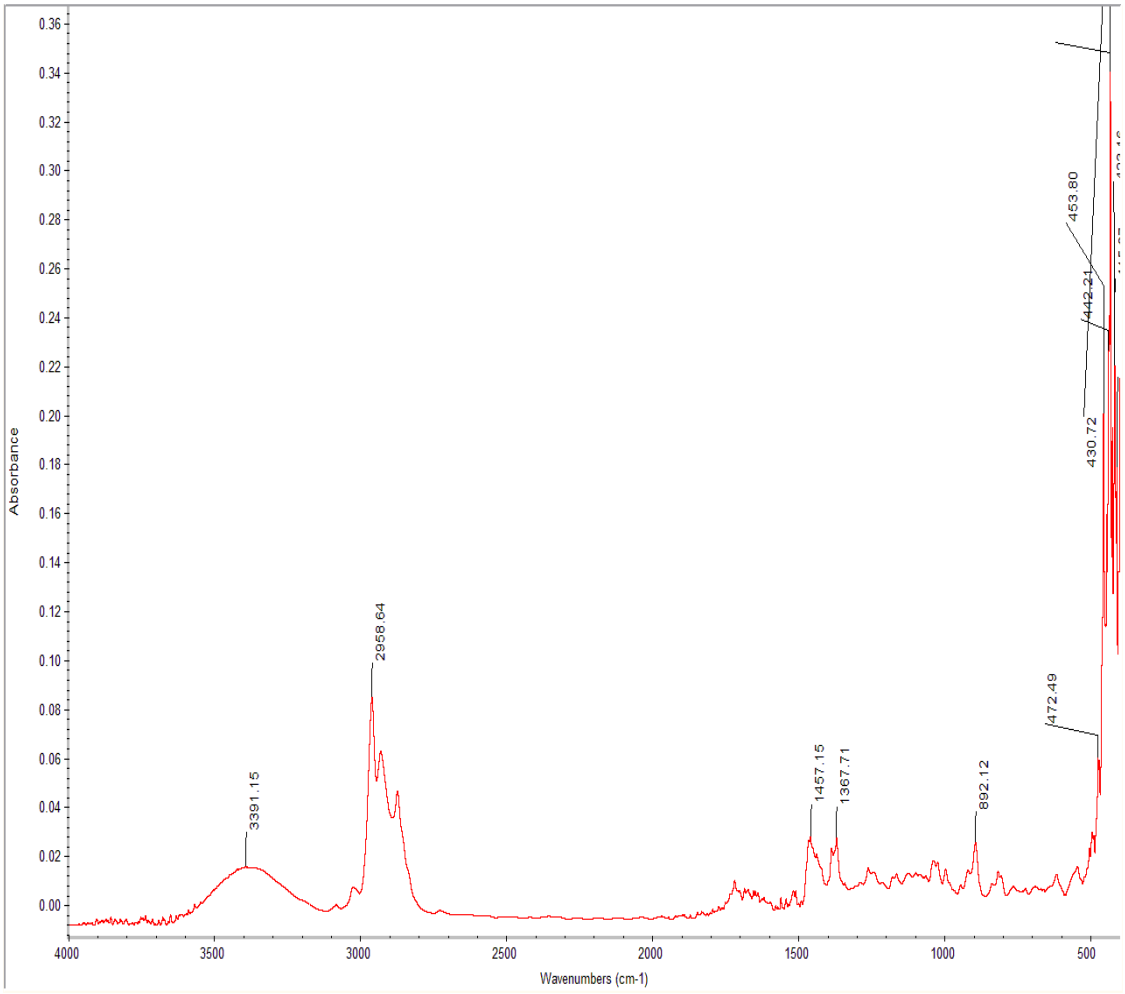

Figure C-1: MMEO FTIR

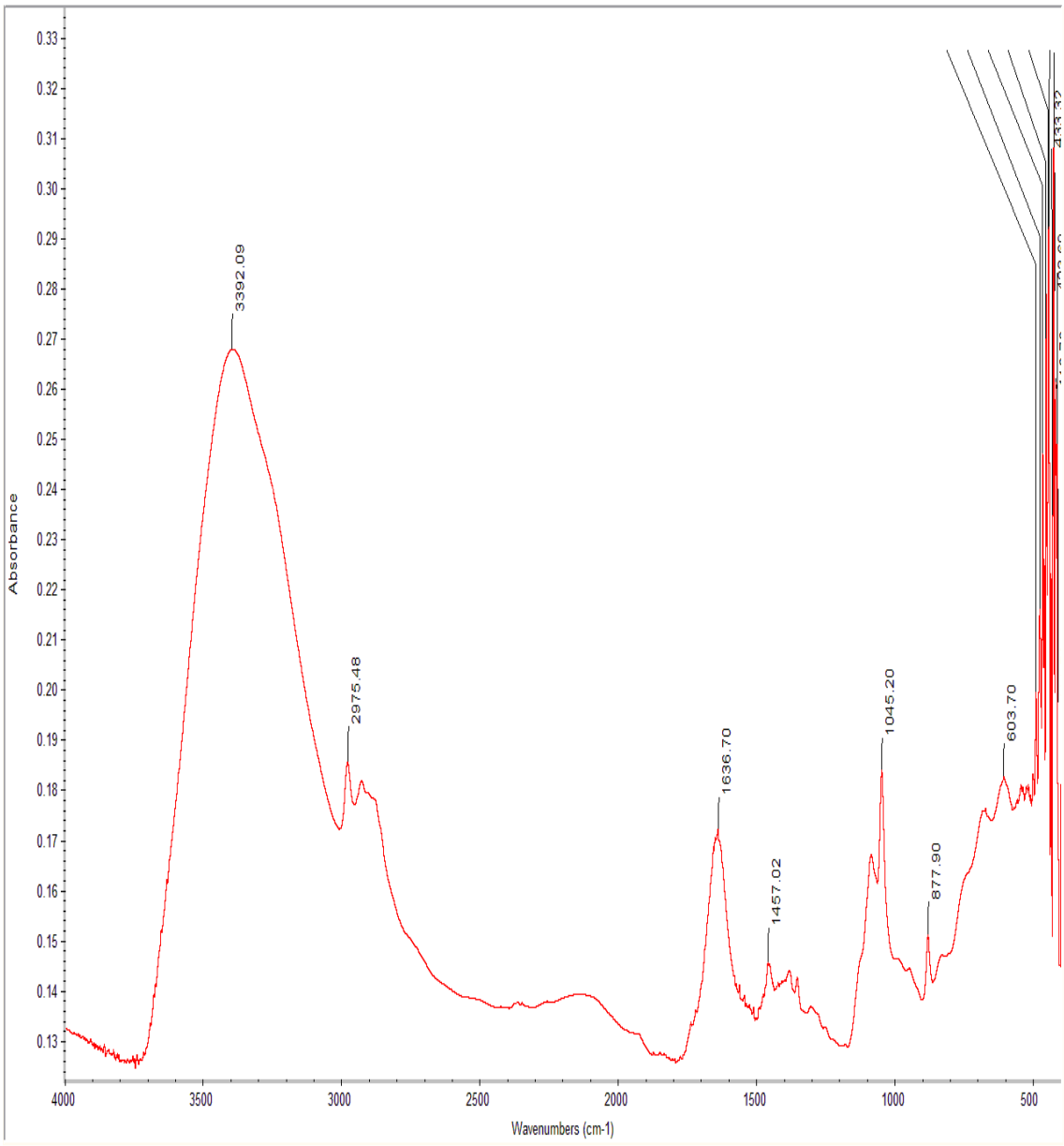

Figure C-2. Emulsion Spectra.